POWER QUALITY IMPROVEMENT USING DSTATCOM IN ALL ELECTRIC PROPULSION SHIPS

A Project Report

submitted by

ANIL MURALEEDHARAN

in partial fulfilment of the requirements
for the award of the degree of

MASTER OF TECHNOLOGY

DEPARTMENT OF ELECTRICAL ENGINEERING
INDIAN INSTITUTE OF TECHNOLOGY MADRAS

JUNE 2022

QUOTATIONS

Whether you're studying electrical engineering or poetry, college is not about maximizing income,it's about becoming a better and more informed observer of the universe. And for me, at least,that what's leads to a more fulfilling life.

JOHN GREEN

DEDICATION

To my family

CERTIFICATE

This is to certify that the project report titled **POWER QUALITY IMPROVEMENT USING DSTATCOM IN ALL ELECTRIC PROPULSION SHIPS**, submitted by **ANIL MURALEEDHARAN**, to the Indian Institute of Technology Madras, for the award of the degree of **Master of Technology**, is a bonafide record of the research work done by him under my supervision. The contents of this project report, in full or in parts, have not been submitted to any other Institute or University for the award of any degree or diploma.

Place: Chennai
Date: June 2022

Prof. Mahesh Kumar
Project Guide
Dept. of Electrical Engineering
IIT Madras, 600 036

ACKNOWLEDGEMENTS

First and foremost, I would like to thank Almighty God for his showers of blessings and helping me overcome the stumbling obstacles.

The completion of my work would not have been possible without the excellent guidance, expertise and motivating support of my guide, Prof. Mahesh Kumar and no amount of gratitude and thanks would be enough. I consider myself fortunate and privileged to work under his supervision and his overwhelming helping temperament has helped me complete my work in time. I would also like to thank Prof. B Kalyan Kumar and Prof. N Lakshmi Narasamma for sharing their valuable knowledge and answering all the puny questions throughout the course of my project. Their unwavering enthusiasm for the subject has been a constant motivator for my work.

I thank Lt Cdr Bobby M Mylady for his invaluable efforts in enlightening me about his studies and offering technical support to the extent possible by clarifying my doubts regarding the existing setup.

My appreciation also extends to my lab colleagues Nakka Pruthvi Chaithanya, Lokesh Nalla, Hariharan, Durga Malleswara Rao, Rajarshi Basu, Tony Thomas, Nimisha M, Abhisek Panda, Leelavathi and Hari Krishna T for motivating and for enlivening the lab with humour.

I also take this opportunity to thank my family members for encouraging me during tough times. I wouldn't have achieved anything without their constant motivation and support.

Last, but not the least, I would like to thank all the Professors of the institute for helping me elevate my knowledge to what it is now. I consider myself lucky to have utilized their wisdom and knowledge.

ABSTRACT

KEYWORDS: Integrated Full Electric Propulsion ; Combatant Vessel; Marine Regulations and Standards; Marine Power System Network; Power Quality; DSTATCOM; SIMULINK.

The expansion of research and development in the field of power electronics have resulted in an extensive usage of efficient power electronic devices for voltage/ frequency conversions. Marine systems are also gradually moving towards power converter based propulsion systems for efficient cruising and voyage. However, the increased usage of power electronic devices in an islanded marine system causes significant current distortions due to the generation of harmonic currents associated with these power electronic devices. Additionally, due to the specific nature of generators used onboard, the current harmonics can cause significant voltage distortions at the point of common coupling, which affects other loads connected to the power network. The situation is even more critical for a combatant marine vessel and hence, inclusion of compensation techniques for power quality improvement is inevitable. Due to the proliferation of disadvantages associated with frequency tuned passive filters, an active filter based compensator has been chosen as the project work for improving the reliability and power quality onboard an electric propulsion ship. A new topology for distribution static compensator (DSTATCOM) applications with nonstiff source is proposed. The proposed topology enables DSTATCOM to have a reduced dc-link voltage without compromising the compensation capability. It uses a series capacitor along with the interfacing inductor and a shunt filter capacitor. With the reduction in dc-link voltage, the average switching frequency of the insulated gate bipolar transistor switches of the DSTATCOM is also reduced. Consequently, the switching losses in the inverter are reduced. Detailed design aspects of the series and shunt capacitors are discussed. A simulation study of the proposed topology has been carried out using MATLAB Simulink platform.

TABLE OF CONTENTS

Page

ACKNOWLEDGEMENTS i

ABSTRACT ii

LIST OF TABLES vi

LIST OF FIGURES viii

ABBREVIATIONS ix

NOTATION x

CHAPTER 1: INTRODUCTION 1

1.1 Literature Review 2

1.2 Objectives 4

1.3 Organisation of Thesis 5

CHAPTER 2: SYSTEM DESCRIPTION 7

2.1 Introduction 7

2.2 Integrated Full Electric Propulsion 8

2.3 Power Generation and Distribution 9

2.4 Marine Loads 12

2.5 Harmonic Cancellation using Passive Filters 13

2.6 Summary 18

CHAPTER 3: COMPENSATOR DESIGN FOR PQ IMPROVEMENT . 19

3.1 Introduction 19

3.2 Instantaneous Symmetrical Component Theory 20

3.2.1 Generation of Reference Source Currents 21

3.2.2 Generation of Fundamental Positive Sequence Components 27

Table of Contents (continued) **Page**

3.3 Computation of Average Load Power, P_{lavg} 29

3.4 Compensator Power Loss Calculation, P_{loss} 30

3.5 Reference Filter Currents Calculation 32

3.6 Methodology for Inverter Control 34

3.7 Interfacing Passive Filter and Shunt Capacitance 35

3.8 Summary 42

CHAPTER 4: SELECTION OF SYSTEM PARAMETERS 43

4.1 Introduction 43

4.2 Selection of Generator Parameters 43

4.3 Selection of Load Parameters 44

4.4 Passive Filter Designing 44

4.5 DC Link Voltage determination, V_{dc} 45

4.6 Selection of DC Link Capacitance, C_{dc} 47

4.7 Maximum Rated Filter Current, I_{f-max} 48

4.8 Maximum Filter Power Rating, S_f 50

4.9 Selection of Hysteresis Band, h 50

4.10 Shunt Capacitor Parameters 51

4.11 Coupling Passive Filter Parameters 52

4.12 Selection of PI Controller Constants, $k_p^{'}$, $k_i^{'}$ 53

4.13 Summary 54

CHAPTER 5: RESULTS AND OBSERVATIONS 55

5.1 Introduction 55

5.2 Results 56

5.3 Summary 63

CHAPTER 6: CONCLUSION 65

6.1 Project Summary 65

6.2 Future Scope 66

REFERENCES 71

LIST OF TABLES

Table	Title	Page
2.1	Characteristics of series and shunt type active filters	17
4.1	Source and load parameters	44
4.2	Active filter parameters	51
4.3	Coupling filter and shunt capacitor parameters	53
5.1	Source and load parameters	56

LIST OF FIGURES

Figure	Title	Page
2.1	A traditional marine system with separate engines	8
2.2	Layout of an IFEP system	9
2.3	A typical CODLAG configuration	10
2.4	Typical combatant maritime power system network [2]	11
2.5	General layout of a VFD fed motor	13
2.6	A typical star connected passive filter configuration	14
2.7	Shunt and series active power filter	16
3.1	A three phase three wire DSTATCOM configuration	20
3.2	Three phase three wire filter configuration	22
3.3	Conventional PI controller for P_{loss} generation	31
3.4	Fast-Acting PI controller for P_{loss}^{mod} generation	32
3.5	Implementation of hysteresis band current controller [31]	34
3.6	DSTATCOM with interfacing passive filter	36
3.7	Static VAR compensator in parallel with a hybrid active filter	38
5.1	DSTATCOM with interfacing passive filter	55
5.2	Source voltage without filter	56
5.3	Source current without filter	57
5.4	Harmonic spectrum w/o filter	58
5.5	Source line voltage and current waveforms with passive filter alone	59
5.6	Harmonic spectrum with passive filter alone	60
5.7	Source line voltage and current waveforms with hybrid filter	61
5.8	Harmonic spectrum with hybrid filter	62
5.9	Reference and actual filter currents	63

5.10 Active filter DC link voltage and current 64

ABBREVIATIONS

IFEP	Integrated Full Electric Propulsion
VFD	Variable Frequency Drive
THD	Total Harmonic Distortion
IGBT	Insulated Gate Bipolar Transistor
MOSFET	Metal Oxide Semiconductor Field Effect Transistor
IGCT	Integrated Gate Commutated Thyristor
DFE	Diode Front End
PI	Proportional and Integral
IMO	International Maritime Organization
MARPOL	The International Convention for the Prevention of Pollution from Ships
LNG	Liquefied Natural Gas
CODLAG	Combined Diesel-Electric and Gas
APMS	Automatic Power Management System
IPMS	Integrated Platform Management System
DA	Diesel Alternator
GTG	Gas Turbine Generator
EDC	Energy Dispatch Centre
PQ	Power Quality
IEEE	Institute of Electrical and Electronics Engineers
VSI	Voltage Source Inverter
DSTATCOM	Distribution Static Compensator
PWM	Pulse Width Modulation
PCC	Point of Common Coupling
EMI	Electromagnetic Interference

NOTATION

English Symbols

L_s	Source Inductance
R_s	Source Resistance
R_f	Damping Resistance
C_f	Passive Filter Capacitance
C_{sh}	Shunt Capacitance
L_f	Passive Filter Inductance
Q_n	Quality Factor
Z_c	Characteristic Impedance
P_{lavg}	Average Load Power
P_{loss}	Compensator Power Loss
k_p, k_i	Conventional PI Controller Gains
$k_p^{'}$, $k_i^{'}$	Fast-Acting PI Controller Gains
V_{dc}	Inverter Input Voltage
C_{dc}	Inverter Input Capacitance
$2h$	Hysteresis Band
S_f	Filter Power Rating
f_s	supply frequency
V_g	Grid RMS Phase Voltage
f_{sw}	Active Filter switching frequency
I_{f-max}	Rated Filter RMS Current
V_{L-pk}	Peak Line Voltage
$V_{CErated}$	Rated Collector Emitter Voltage
Q_L	Load Reactive Power

Greek Symbols

ψ_+	Angle between fundamental phase voltage and current
β	An indicator of amount of reactive power compensation required
ω_r	Resonant angular velocity

CHAPTER 1

INTRODUCTION

The electric propulsion concept is primarily based on principle of employing either a partially or fully integrated Electric power system for both propulsion and ship's auxiliary weapons services. This is achieved through first generating much larger capacity Electric power using parallel connected prime movers such as diesel/gas/steam engines coupled with diesel generating (DG) sets and then employing this integrated pool of Electric power to meet various power requirements of the ship. These requirements include shaft power for ship's propulsion (through an electric motor), power for weapons and radar systems, power for auxiliary and other support systems services. The surplus Electric power in any of the system can be diverted to other systems as and when required. This concept ensures that the prime movers are always optimally loaded at their most energy efficient operating regimes. The reduction gearbox as well as substantial part of mechanical shaftlines employed in conventional or mechanical propulsion system is no longer required [1]. Since inception, Integrated Full Electric Propulsion (IFEP) ships are known to have enhanced performance and greater advantages over conventional propulsion ships viz. better maneuverability, higher efficiency, easier controllability and faster response [2]-[3].

However, these Full Electric Propulsion Ships employ 12/18 pulse diode front end Variable Frequency Drives (VFD) for driving the propulsion motors [2], which utilizes the principle of high-speed switching of solid-state devices like Insulated Gate Bipolar Transistors (IGBT), Metal Oxide Semiconductor Field Effect Transistors (MOSFET), Integrated Gate Commutated Thyristors (IGCT) etc [3]. These non-linear components cause significant generation of harmonics [4], causing non-sinusoidal currents being drawn from the shipboard generators. Since shipboard generators have higher source impedence (15-20%) as compared to conventional shore generators (4-5%) [2], there will be significant voltage distortion due to generation of current harmonics and can

affect other loads connected to the generator. The mentioned cause can have devastating effect onboard a warship as the other prominent loads connected are weapon/ radar systems, which might lead to deteriorated performance of such critical systems and can have fatal effects at the time of war, until unless good performance efficient input filters are designed for individual systems connected to the grid.

1.1 Literature Review

Understanding the setup of the current system with various motor types was the key issue at hand because the proposed filter design was meant for a navy warship. Chetan K et al.[1] went over the various configurations that are available for propulsion and the steps necessary to adopt it onboard Indian naval ships. Dinesh Kumar et al. [2],C. Hodge [3], Y.M. Terriche et al. [4], B.D. Reddy et al. [5], J Mindykowski [6] explained in detail the configurations of marine power system network, the power quality problems associated with electric propulsion ships, PQ mitigation techniques etc. V. Arcidiacono et al. [7] discussed the configuration of full electric propulsion ships, as well as the power system network and onboard controls. IEEE Stds [8]-[9], which gave an insight into the standards required for electrical installation onboard ships and for harmonic control in electric power systems, respectively, were also referred to for understanding the various standards associated with the design and installation of active filters onboard.

S.V. Giannoutsos et al. [10], S. Puthalath [11] address the possibilities of using several types of passive filters to reduce Total Harmonic Distortion (THD) onboard marine systems in depth. The authors also discussed how to reduce harmonics to acceptable levels using several shunt linked passive filters (LC filters) adjusted to respective harmonic frequencies, as described in [8]-[9]. Even though these filters can reduce THD to tolerable levels, they are heavy, take up a lot of space, and provide poor power quality control, among other drawbacks. Furthermore, at low loads, passive filters can cause overcompensation and thus over-voltages, necessitating efficient design across a wide load range. N.K. Bett et al.[12], V.F. Corasaniti et al. [13] give detailed explanations

of the advantages and disadvantages of using passive/ hybrid power filters for harmonic cancellation and reactive power compensation.

To address the aforementioned shortcomings in the passive filter design, a new design is offered in which the passive filters are replaced with active filters, allowing for better control of current harmonics and hence good overall power quality. H. Akagi et al. [14]-[15]-[16], R. Inzunza et al. [17] examined several active filter configurations available for reducing source current/voltage THDs. They also detailed the benefits of active filters over passive filters, the benefits of hybrid filters over both, and the distinctions between series and shunt active power filters, among other things. A shunt active power filter was discovered to be the best alternative for our current system requirements. These shunt active power filters are attached to the VFD's source side and make use of high-speed switching devices such as IGBTs and MOSFETs. They can generate currents/voltages in phase opposition at harmonic frequencies, allowing the source generator to generate sinusoidal current waveforms. The load side harmonics are monitored, and a feedback loop is provided to the filter unit, which provides instant filtering [14], which varies substantially depending on the torque/speed regimes applied via VFDs and propulsion motors. Overall THD is predicted to be significantly decreased, ensuring greater power quality to other connected loads. As a result, the size of input filters in other loads, such as radar and missile systems, can be reduced. Additionally, 12/ 18 pulse diode front end can be replaced with transformer-less 6 pulse diode front end VFDs, as explained in [5], thereby reducing the overall size of VFDs as well.

However, to achieve perfect compensation, these filters require a well-designed control system. J.L. Afonso et al. [18] have described in detail one common control theory, dubbed pq theory, as well as its implementation and benefits. However, E.H. Watanabe et al. [19] highlighted some of the issues with pq theory, therefore another control theory, called instantaneous symmetrical component theory, was researched in depth to comprehend the ideas and benefits of implementation for an active filter control system. Mahesh Kumar et al. [20]-[21]-[22], U.K. Rao et al. [23], N.M. Ismail et al. [24], J. Suma et al. [25], Chandan Kumar et al. [26]-[27] provided an insight on design

and implementation of an active filter as compensator for harmonic cancellation and reactive power compensation using instantaneous symmetrical component theory. The authors have explained several design modifications to improve DSTATCOM performance under various source and load parameter regimes. Additionally, Mahesh Kumar et al. [28] explained the design of a fast-acting PI controller for maintaining constant DC link voltage at the inverter source capacitor and its advantages over a conventional PI controller. Also, it was learned from D.M. Ingram et al. [29], Pan Ching-Tsai et al. [30], M. Kale et al. [31] that a hysteresis band current controller is an ideal option for generating the filter currents calculated using instantaneous symmetrical component theory. The authors discussed the design and implementation of hysteresis band current controller and the various advantages and disadvantages associated with the controller.

Following the design of the control system, a coupling filter as a current smoothing circuit is required. S. Jayalath et al. [32], Marco Liserre et al. [33], Chandan Kumar et al. [34], R. Pena-Alzola et al. [35], A. Reznik et al. [36] have discussed and derived the mathematical expressions for an effective LCL filter as a coupling device to reduce the current ripple and to smoothen the filter current. However, the topology with an active filter alone will result in increased DC link voltage as explained by S.B. Karanki et al. [37] and L.Wang et al. [38]. The authors have further explained the advantages of using a hybrid topology with a shunt capacitor which can give better results. In addition, various losses induced by the compensator circuit must be computed. The methods for calculating various losses of an IGBT were explained by G. Feix et al. [39].

1.2 Objectives

The suggested concept is expected to overcome the limitations of passive filters in terms of improving THD and compensating reactive power as discussed. Based on this following objectives are considered.

- Design an active filter, along with its control system, for the non-linear VFD driven propulsion motor loads used onboard electric propulsion ships.
- Design an effective passive filter to be used in series with the active filter to make

the combination function as a hybrid filter. Further, design shunt capacitor to be used in shunt with the hybrid filter.

- Simulate the designed compensator to evaluate its performance with the source and load parameters of the existing system.

The proposed filter is projected to perform better and superior than a passive filter system because hybrid filters can function efficiently across a large load range. An efficient design is conducted utilising the original source and load characteristics, and the same is simulated using MATLAB Simulink to assess the suggested filter's performance.

1.3 Organisation of Thesis

Chapter 2 gives a general overview of the system, covering the many methods of propulsion, the reasons for the steady move from mechanical to electrical propulsion, the layout of the marine power system, and the numerous types of maritime loads. This chapter also covers the fundamentals of using frequency tuned passive filters onboard for harmonic cancellation and reactive power compensation. It also gives an overview of the many types of active filters and their distinct qualities.

Chapter 3 describes DSTATCOM's operation for generating harmonic currents from filter reference currents utilising instantaneous symmetrical component theory. This chapter also covers the theoretical components of filter parameter computing, such as power loss computation, inverter control technique for filter current production, and the benefits of utilising a hybrid filter in shunt with a capacitor.

Chapter 4 deals with the design of components for optimal filter performance. This includes designing the inverter source capacitor, calculating the maximum filter current required for ideal compensation, determining the hysteresis band based on the maximum allowed current ripple at the filter output, computing the hybrid filter and shunt capacitor parameters and designing PI controller to maintain constant DC link voltage.

Chapter 5 discuss the simulation results, including observations and conclusions

drawn from the simulation data.

Chapter 6 summarises the project work by listing the benefits of the proposed system as well as the project's future scope, followed by references.

CHAPTER 2

SYSTEM DESCRIPTION

2.1 Introduction

Because of the long-term influence on our environment, greenhouse gas emissions, climate change, and global warming have been hot topics of concern in many countries, including India. One of the main causes of these emissions is the combustion of fossil fuels, and different national/international bodies throughout the world have been working hard to lower overall greenhouse gas footprint through various policies and politics. Many strict laws and guidelines for power plant selection have been put in place to achieve this, including the use of cleaner power sources, burning good fuel, and enhancing power plant efficiency to achieve improved production. The marine sector alone is responsible for around 15% of global Nitrogen Oxide (NOX) emissions and 3% of global carbon monoxide emissions [2] and is likely to rise as governments around the world become more reliant on the marine sector for transportation and other services.

The most popular source of power in the marine industry is diesel engines, which are used for both electric power generation and propulsion [5]. Their fuel utilisation factor, on the other hand, is close to 40% [2], implying that the bulk of the energy created is lost as heat dissipation through exhaust. Through the International Convention for the Prevention of Pollution from Ships, the International Maritime Organization (IMO) has begun to impose more limitations on ships in recent years in order to enhance fuel efficiency and reduce heat signatures (MARPOL). The shipping industry has been gradually moving toward Integrated Full Electric Propulsion systems to improve the fuel efficiency of onboard engines [2].

2.2 Integrated Full Electric Propulsion

Figure 2.1 depicts a traditional marine system with separate engines for propulsion and electric power generation. Because these massive engines are mounted in the midships for stability reasons, long shafts and gearbox assemblies are used to connect the engines to the propellers, which are mounted aft. Long shaft lengths can produce excessive noise and vibration, as well as balancing concerns [2], which are incompatible with a combatant vessel design. The fuel economy of such a ship's engines is fairly minimal, as the engines are mostly used at low/medium loads.

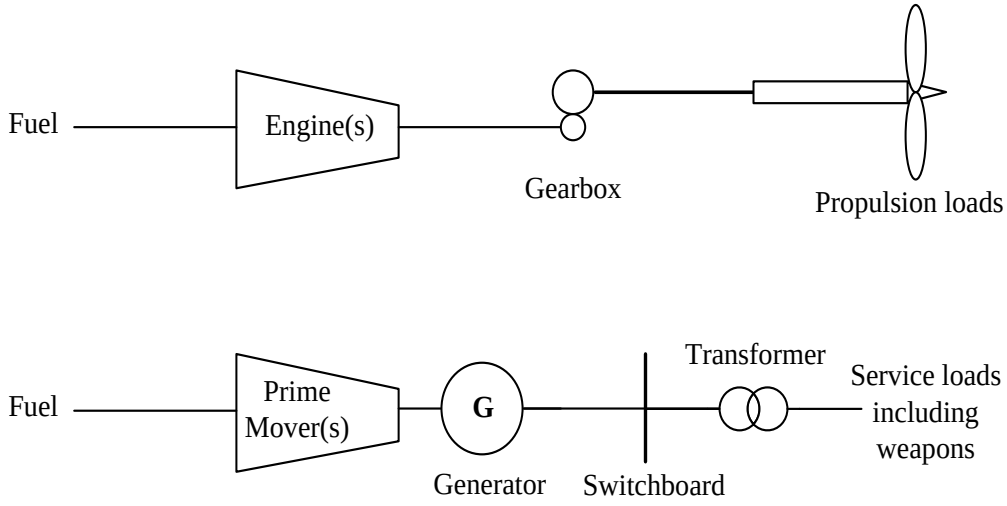

Fig. 2.1: A traditional marine system with separate engines

Marine propulsion systems have gradually evolved from conventional direct engine driven propulsion systems to VFD fed motor-driven propulsion systems in recent years, due to advances in power electronics research and development. To this end, maritime systems all over the world have begun to take use of the benefits of an integrated system, which employs two or more engines that can provide both electric and propulsive power concurrently [3]. Because they use common engines for propulsion and electric power generation, these systems have higher efficiency and fuel consumption. The layout of an IFEP System is shown in Fig. 2.2.

Several non-combatant vessels, such as cruise ships, icebreakers, LNG carriers, fishing vessels, reefer containers, and others, have already been converted from traditional propulsion systems to integrated electric propulsion systems due to the bene-

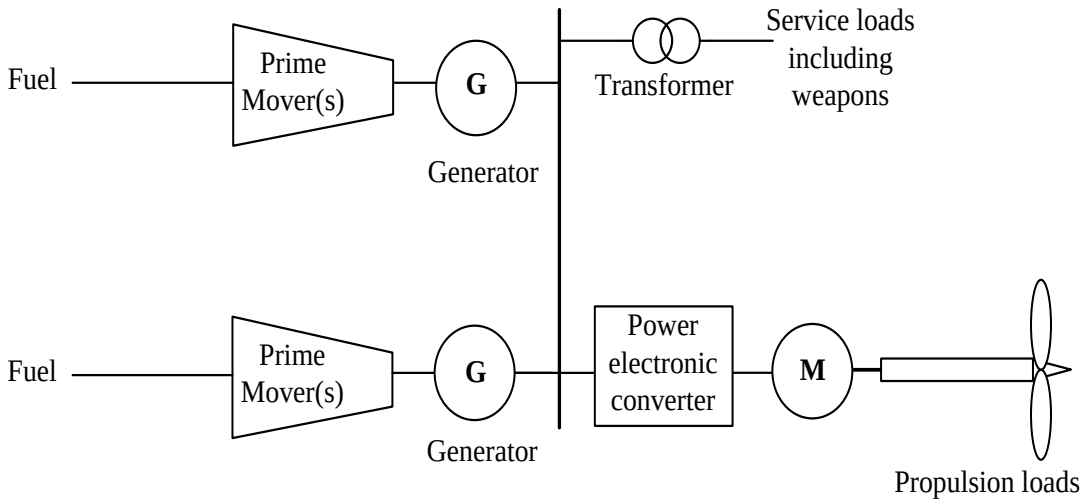

Fig. 2.2: Layout of an IFEP system

fits of IFEP [7]. Combatant vessels, such as frigates, destroyers, and aircraft carriers, differ from non-combatant counterparts in that they are extremely dense systems with large engines and technology-intensive equipment such as radar, weapon systems, complex sensors, and communication systems, which are frequently provided in duplicate for redundancy, to name a few. These military vessels are designed for varied speed regimes with very low acceptable heat and noise characteristics when compared to non-combatant vessels. When compared to a ship using a traditional propulsion system, an IFEP is thought to be more fuel efficient with lower infrared and acoustic signals [2]. A combination of diesel-electric and gas (CODLAG) propulsion is also used due to the changing speed, torque, and power needs of a military vessel. CODLAG arrangement is used by ships such as the Type 45 destroyers of the United Kingdom and the F125 German frigates [1]. The layout of a typical CODLAG arrangement is shown in Fig. 2.3. The Indian Navy has also made orders for electric propulsion ships, one of which will be commissioned later this year, owing to the expected proliferation of benefits.

2.3 Power Generation and Distribution

A ship's power system network is distinct from a standard on-shore power network in that it is an isolated system with dedicated generators and loads situated close together

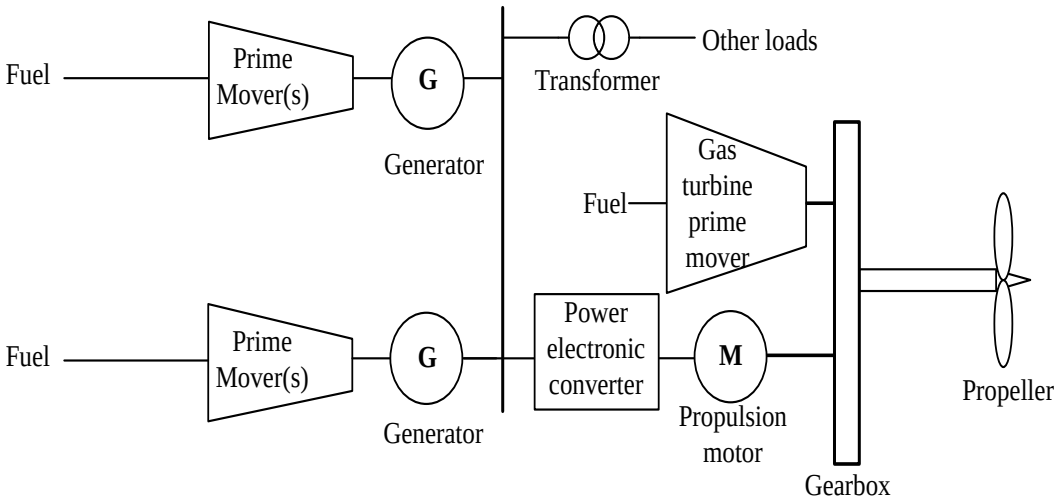

Fig. 2.3: A typical CODLAG configuration

with short length feeders. The generated energy is supplied locally to many high-power loads that require a consistent and high-quality supply. An Automatic Power Management System (APMS) or an Integrated Platform Management System (IPMS) can regulate the complete power network from a master console or one of the slave controls (IPMS). An APMS's multiple tasks include automatic starting, paralleling and loading of DAs, load sharing, and black out start of DAs [7]. Fig. 2.4 shows the layout of a maritime power system network.

The principal source of power onboard is a synchronous generator, which is powered by a diesel or gas prime mover and is thus known as a Diesel Alternator (DA) or Gas Turbine Generator (GTG). To reduce the short circuit current in the event of a ground failure, these generators are star wound with the neutral point connected to the ship's hull through a high impedance circuit. Because the load cannot reach the neutral point, all three phase generators and loads are coupled in a floating neutral configuration. Additionally, the internal impedance of generators and transformers combined is generally much higher (almost 15-20%) when compared to its onshore counterparts (3-5%) [2]. Because power availability is critical for a military vessel, the aggregate MW rating of all generators will be around double the maximum demand, providing redundancy and improving reliability. The generators are distributed throughout a combatant vessel to provide redundant power in the event of a missile or torpedo attack on one

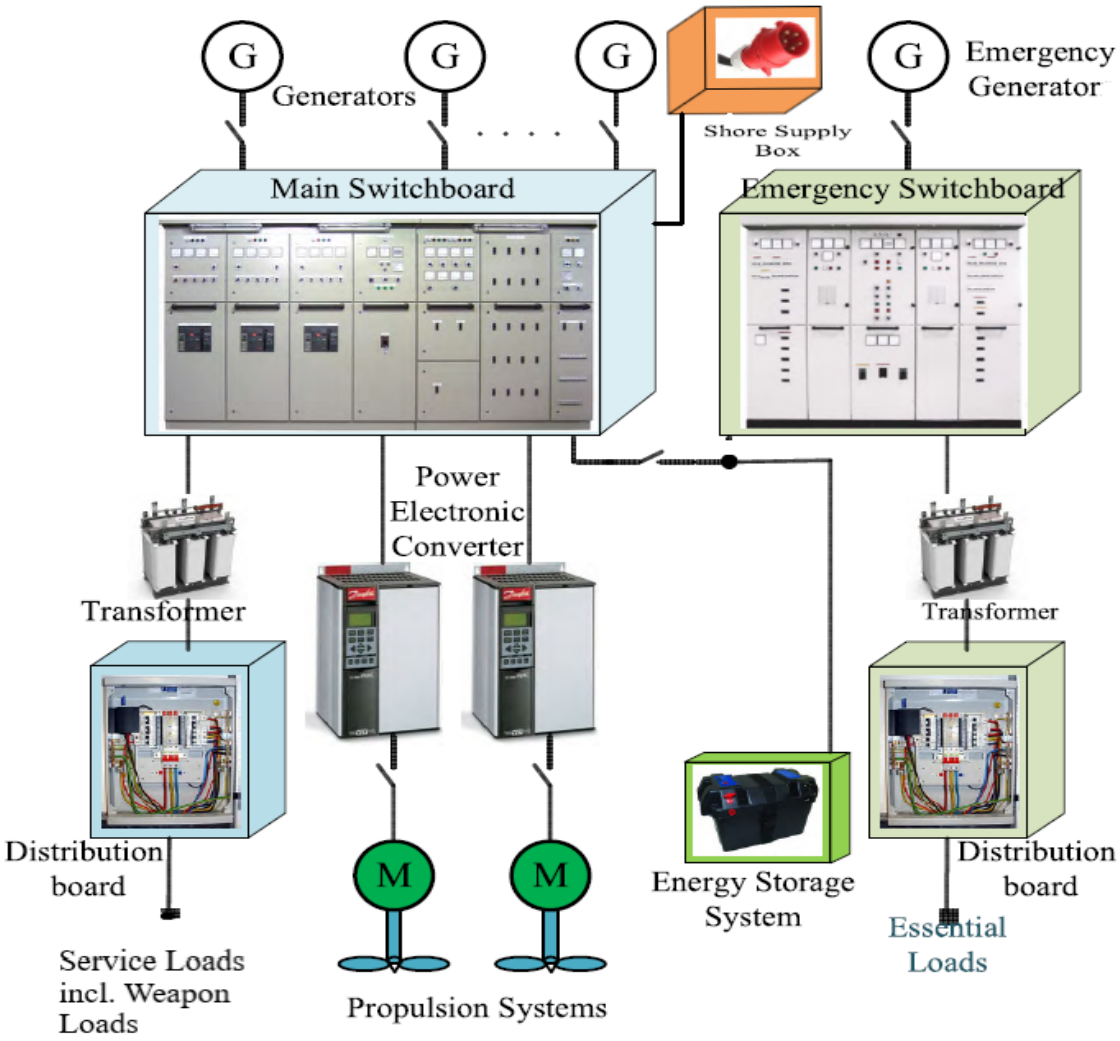

Fig. 2.4: Typical combatant maritime power system network [2]

section of the ship.

A supply breaker connects each generator to a specific area of the main switchboard, with a bus-coupler breaker linking numerous parts of the same switchboard and inter-connecting breakers connecting separate switchboards. Two or more main switchboards, as well as an isolated emergency switchboard, will be powered by an emergency generator and connected to critical loads such as navigation, communication and steering gear. Except for armament equipment, which is fed separately from weapon switchboards, and propulsion motors, which are directly fed from the main switchboard through power converters, electricity from the main switchboard is fed to various loads via energy dispatch centres (EDC). There are numerous secondary supplies available

in addition to the primary supply, which are generated from the primary supply using rectifiers and/or converters. Batteries are also given for backup of vital equipment such as communication equipment, black start of DAs, and so on [2]-[6].

2.4 Marine Loads

All the loads of a marine system are concentrated in a relatively small region, as defined in Section 2.3, and thus all the loads are connected with small length feeders [2]. All loads onboard a combatant vessel are colour coded in descending order of criticality, based on the criticality of equipment for floating and fighting capability, as blue, green, red, white, and yellow. Marine loads on board a combatant vessel can be divided into three categories.

(a) **Propulsion Load**

Onboard an electric propulsion ship, this is the largest power consumer [7]. A power converter feeds an inverter-duty propulsion motor, most frequently an induction type, which is attached to the propeller, which determines the ship's ground speed. The general layout of a diode front end VFD fed motor is shown in Fig. 2.5. Because a motor is significantly lighter than an engine, it can be housed in the aft compartments, avoiding the necessity of long shafts and the problems that come with them [3]. Due to the non-linear nature of power converters, these VFDs can generate substantial current harmonics at the source, causing power quality and stability difficulties in the distribution network [6]. Due to the high source impedance of a marine generator, current harmonics can produce severe voltage distortion, resulting in power quality and system dependability difficulties [2]. Other loads connected to the same source suffer greatly from the voltage distortion generated by the power converters. If the source is not compensated, all other connected loads must have well-designed input filters to ensure high power quality.

(b) **Weapon and Sensor Load**

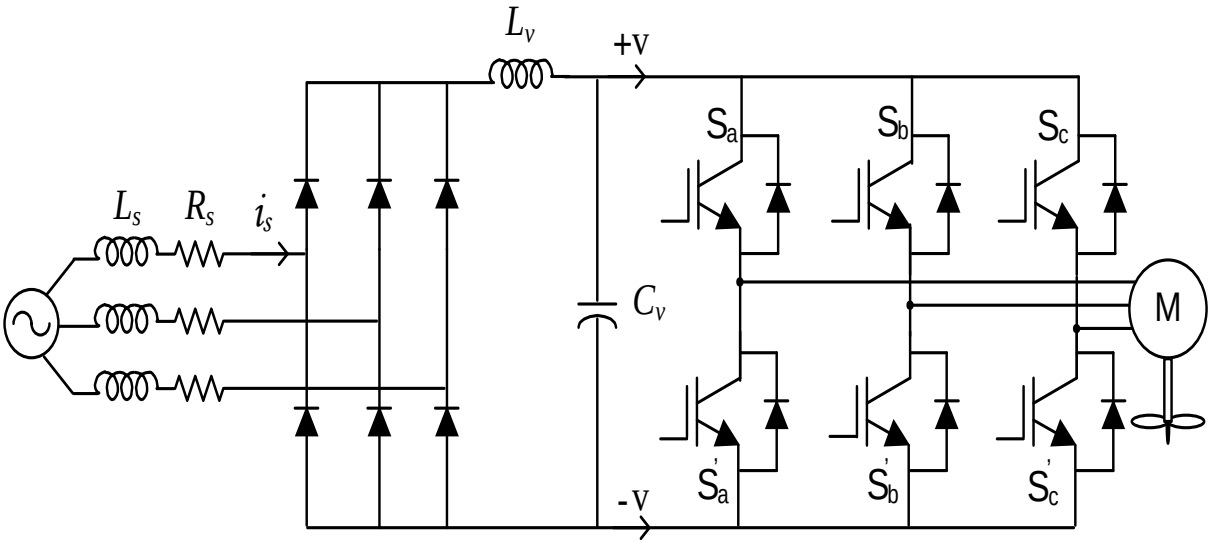

Fig. 2.5: General layout of a VFD fed motor

Due to its specialised function in safeguarding the security of the country it represents, weapon and sensor loads are one of the most critical loads onboard a combatant vessel. For weapon and sensor equipment, good power quality is required, hence power quality issues produced by the propulsion system must be addressed to make the task of the weapon system integrator easier.

(c) **Service Load**

Air conditioning, refrigeration, general lighting and ventilation, firemain system, galley equipment, domestic supply, and other low-power loads are examples of service loads. Despite the fact that these loads are not particularly significant, the availability of a reliable power supply is required for improved system performance.

2.5 Harmonic Cancellation using Passive Filters

Harmonic cancellation and maintaining good power quality is essential for a combatant electric propulsion vessel for following reasons [4].

- To avoid damage to power system components

- To minimize blackouts
- To avoid heating of electrical equipment like transformers
- To avoid false tripping and failure of circuit breakers
- To avoid malfunctioning of measurement devices

The use of 12 pulse converters in a VFD is the major step in reducing harmonics [5]. THD is reduced as a result. However, as recommended by [8]-[9], this does not reduce THD values to acceptable levels. Adding AC line reactors, DC link reactors (chokes), and frequency adjusted passive filters are some of the usual approaches for further reducing THD, with frequency tuned filters being commonly employed for most marine systems [10]. A passive filter has two main functions: desired reactive power compensation and harmonic current absorption caused by the load [13]. They are low-cost devices with a straightforward design and minimal maintenance [12]. These filters are connected in parallel to the non-linear load on the AC side and are adjusted to a specific resonant frequency. It is made up of inductors and capacitors linked to a three-phase line in a star or delta configuration, and it serves as a low-impedance channel for tuned frequency currents. To avoid resonance with the source, it is vital to consider the source inductance while building passive filters [10]. The general circuit layout of a star linked frequency tuned series passive filter is shown in Fig. 2.6.

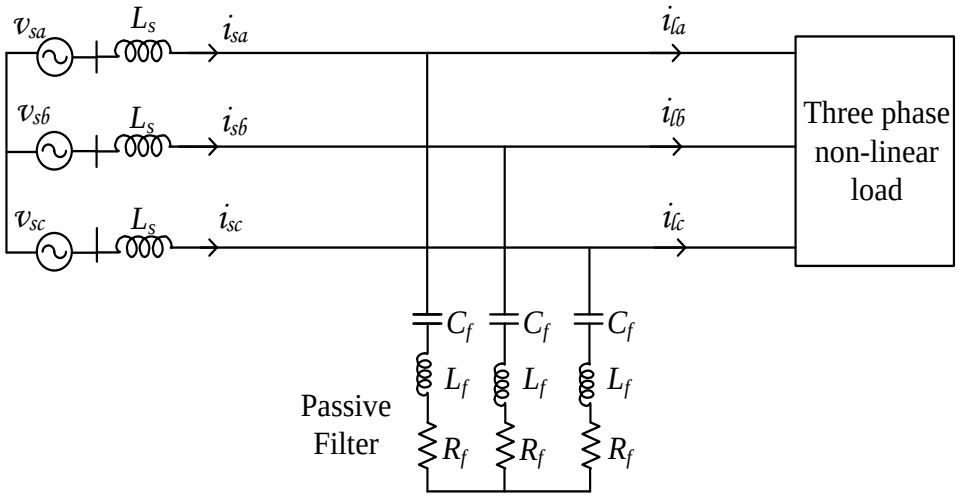

Fig. 2.6: A typical star connected passive filter configuration

Initially, value of capacitance is selected for compensating reactive power in part or full, which is given in the following equation [11],

$$C_f = \frac{Q_f}{3 \times 2\pi f_s V_g^2} \tag{2.1}$$

where, Q_f is the amount of reactive power compensated by the passive filter, f_s is the supply frequency and V_g is the per phase grid voltage. Once the filter capacitance value is determined, the inductance value can be computed for a tuned harmonic resonant frequency, ω_0, as [11],

$$L_f = \frac{1}{\omega_0^2 C_f} \tag{2.2}$$

Also, for a quality factor, Q_n, the value of series resistance, R_f can be determined from (2.3). Even though reduced Q factor gives improved performance over multiple harmonic frequencies, this will result in increased losses in the circuit due to higher resistance value. Moreover, the performance of the filter at the specific tuned frequency will reduce. Hence, it is clear that the resistance value decides the sharpness of tuning and limits harmonic current flowing in the filter [11].

$$R_f = \frac{\omega_0 L_f}{Q_n} \tag{2.3}$$

The characteristic impedance of the passive filter also plays a significant role in the filtering performance. The computation of characteristic impedance is as given in (2.4). The value of characteristic impedance should be as low as possible to improve the filtering performance. However, this implies a larger capacitance value, which makes the system bulky and expensive and results in large reactive power flow through the filter [17].

$$Z_c = \sqrt{\frac{L_f}{C_f}} \tag{2.4}$$

Even though, multiple frequency tuned passive filters seem to be an ideal option for harmonic cancellation, it has the following disadvantages [12].

- can filter only the frequency they are previously tuned for
- operation can not be limited to a certain load and hence the range of operation is

relatively small

- can overload the utility system
- dependent on source impedance
- can cause parallel resonance between power system and filter
- performance degradation and detuning due to aging of components
- resonance due to interaction with other loads leading to unpredictable results.

Due to the numerous drawbacks of a frequency-tuned passive filter, an active filter is seen to be the best solution for a marine power system because of its improved characteristics and superior performance over a large load range [15]. Based on the type of filters employed, active filters are recognised to offer the best performance for harmonic cancellation, reactive power compensation, or voltage regulation. As shown in Fig. 2.7, active filters can be shunt or series. Table 2.1 [14] lists the features of series and shunt active power filters.

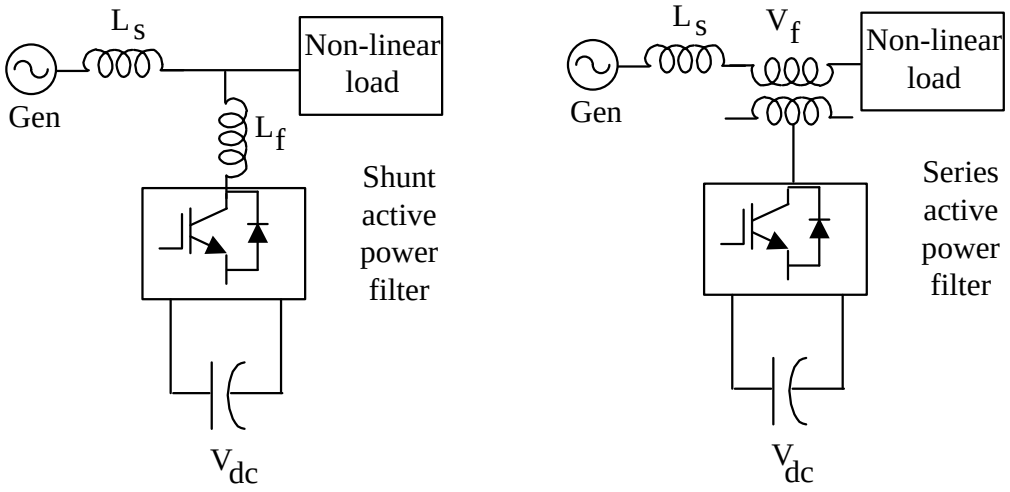

Fig. 2.7: Shunt and series active power filter

Because marine propulsion loads are induction kinds that generate a lot of current harmonics, shunt type voltage fed inverters were chosen because they are perfect for pure harmonic cancellation and reactive power compensation. The compensating current generated by the shunt active filters suppresses the ac side current harmonics, resulting in a pure sinusoidal source current waveform.

Table 2.1: Characteristics of series and shunt type active filters

Configuration/ Specs	**Series Type**	**Shunt Type**
Power Circuit	Voltage fed PWM inverter connected in series with the load	Voltage fed PWM inverter connected in parallel with the load
Type of Source	Voltage source	Current source
Primary role	Voltage regulation	Current harmonic Suppression
Secondary Role	Voltage Harmonic Suppression, sag/swell mitigation	Reactive power compensation
Applications	Non-linear capacitive loads	Non-linear inductive loads

However, the compensation performance of any active filter depends on the voltage rating of dc-link capacitor. In general, the dc-link voltage has much higher value than the peak value of the line-to-neutral voltages. This is done in order to ensure a proper compensation at the peak of the source voltage. In [24], Nafih M Ismail et al. have suggested the dc-link voltage should be greater than or equal to 1.6 times the phase voltage of the system for distortion-free compensation. When the dc-link voltage is less than this limit, there is insufficient resultant voltage to drive the currents through the inductances so as to track the reference currents. Reference value of the dc-bus capacitor voltage mainly depends upon the requirement of reactive power compensation of the active power filter. The primary condition for reactive power compensation is that the magnitude of reference dc-bus capacitor voltage should be higher than the peak of source voltage at the PCC. Due to these criteria, many researchers have used a higher value of dc capacitor voltage based on their applications. With the high value of dc-link capacitor, the voltage source inverter (VSI) becomes bulky and the switches used in the VSI also need to be rated for higher value of voltage and current. This, in turn, increases the entire cost and size of the VSI [37]-[38].

A new hybrid DSTATCOM topology has been proposed in this project, which has the capability of compensating the load at a lower dc-link voltage under nonstiff source. The topology consists of two capacitors, one is in series with the interfacing inductor of the active filter and the other is in shunt with the active filter. The series capacitor enables reduction in dc-link voltage while simultaneously compensating the reactive

power required by the load, so as to maintain unity power factor without compromising DSTATCOM performance. The shunt capacitor, maintains the terminal voltage to the desired value in the presence of source impedance [37]. The ultimate aim with a hybrid arrangement is to improve the performance of passive filters and to reduce the size of active filters [15]-[17].

2.6 Summary

The basic principles of propulsion types in the maritime sector, particularly onboard combatant vessels, were introduced in this chapter, as well as the reasons behind the steady change from conventional to electric propulsion. The fundamentals of power system network layout and setup, as well as the particular of maritime generators and loads, are briefly reviewed. This chapter discusses the use of passive filters as compensators, as well as the benefits of using active filters for reactive power compensation and harmonic cancellation. Further, the advantages of using a hybrid filter in lieu of active filters to improve filter performance is also discussed. The next chapter will go into the detailed explanation and control ideas for hybrid filters.

CHAPTER 3

COMPENSATOR DESIGN FOR PQ IMPROVEMENT

3.1 Introduction

As a controlled source for creating harmonic currents required for the load, DSTATCOM has been known to be one of the best custom power devices [17] for current harmonic suppression. These filters generate equal but opposite harmonic currents, reducing source current harmonics. For the creation of source reference currents, the filter comprises of an inverter unit with an associated control system. Because the inverter unit's DC link capacitor is responsible for load reactive power compensation, the filter unit is an excellent choice for reactive power compensation as well as harmonic current suppression. A generic circuit configuration of a typical DSTATCOM is shown in Fig. 3.1. For reference current generation, the following two main theories are often utilised [20].

(a) Instantaneous Reactive Power Theory (p-q theory)

(b) Instantaneous Symmetrical Component Theory

Some of the benefits proposed in the literature for p-q theory include excellent dynamic responsiveness, good performance with certain sub-harmonics like flicker, and creation of proper values of compensatory voltage and current [18]. However, there is some evidence that p-q theory causes the formation of hidden currents, which are additional harmonics in the current components that were not present in the original current waveform [19]. Furthermore, p-q theory requires every instantaneous transition from abc to $\alpha - \beta$ frame for the generation of compensating currents, which is computationally demanding. Also, in p-q theory, the notion of reactive power in the $\alpha - \beta$ domain is

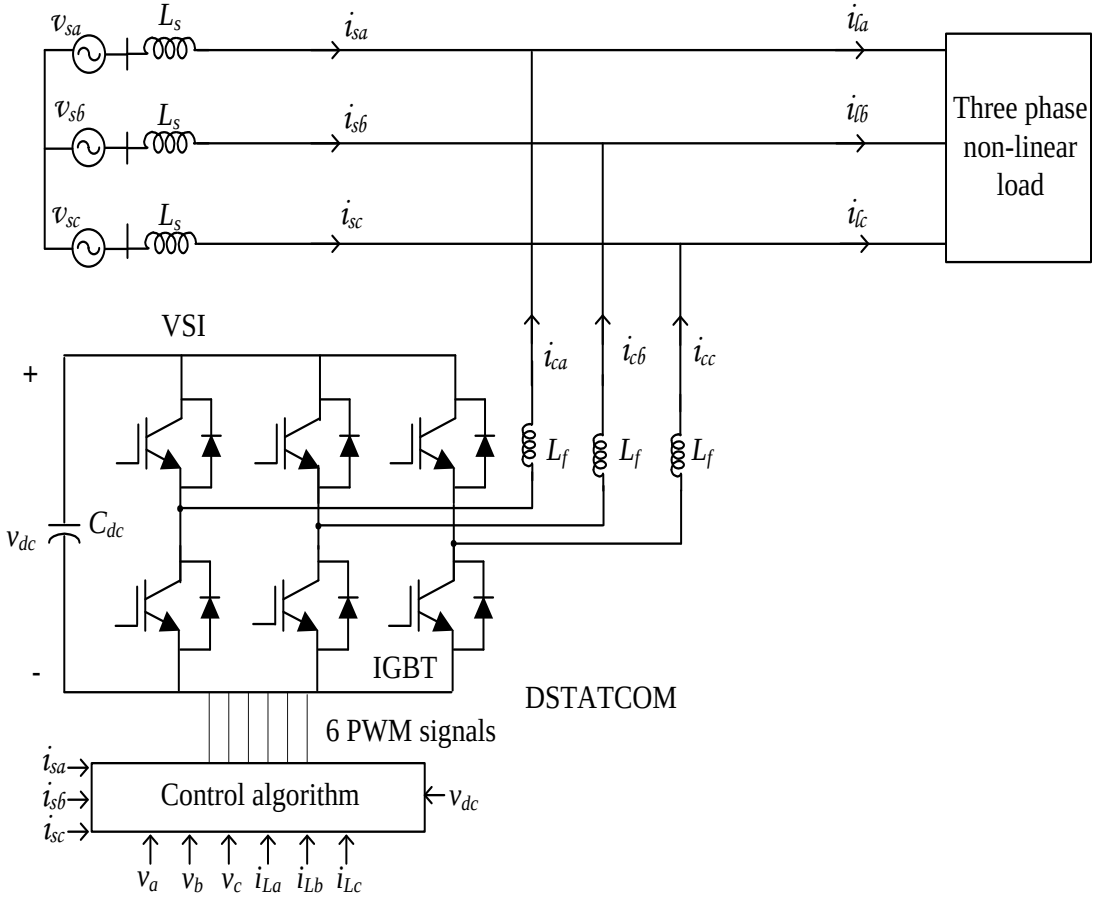

Fig. 3.1: A three phase three wire DSTATCOM configuration

ambiguous and does not reflect actual reactive power. In addition to the advantages anticipated for p-q theory, instantaneous symmetrical component theory is straightforward to formulate and devoid of any reactive power ambiguity [23]. As a result, for reference current generation in the current design, instantaneous symmetrical component theory is employed, as detailed in the following paragraphs.

3.2 Instantaneous Symmetrical Component Theory

CL Fortesque introduced symmetrical components in 1918 to convert an unbalanced n-phase system into a balanced system of n related phasors of equal amplitude with the

same phase angle differences between the n phasors of each set. Instantaneous symmetrical components are frequently employed because they indicate instantaneous changes in supply voltages/currents, making it simple to identify power system faults. The zero, positive, and negative sequence components of instantaneous voltage and current can be resolved as follows,

$$\begin{bmatrix} \overline{v}_{a0} \\ \overline{v}_{a+} \\ \overline{v}_{a-} \end{bmatrix} = \frac{1}{3} \begin{bmatrix} 1 & 1 & 1 \\ 1 & a & a^2 \\ 1 & a^2 & a \end{bmatrix} \begin{bmatrix} v_a \\ v_b \\ v_c \end{bmatrix} \tag{3.1}$$

$$\begin{bmatrix} \overline{i}_{a0} \\ \overline{i}_{a+} \\ \overline{i}_{a-} \end{bmatrix} = \frac{1}{3} \begin{bmatrix} 1 & 1 & 1 \\ 1 & a & a^2 \\ 1 & a^2 & a \end{bmatrix} \begin{bmatrix} i_a \\ i_b \\ i_c \end{bmatrix} \tag{3.2}$$

Here, $\overline{v}_{a+}$, $\overline{v}_{a-}$ and $\overline{i}_{a+}$, $\overline{i}_{a-}$ are complex time varying quantities of instantaneous voltages and currents respectively with positive and negative sequence phasors rotating in opposite direction with each other. In the above (3.1) and (3.2), a is a complex operator given by $a = 1\angle 120^\circ$ and $\overline{v}_{a0}$ and $\overline{i}_{a0}$ are stationary voltage and current phasors with real magnitude.

3.2.1 Generation of Reference Source Currents

As explained in Chapter 2, the system under consideration is a three phase, three wire system feeding a non-linear load, as shown in Fig. 3.2. The following equation for instantaneous source currents is satisfied for three phase three wire system.

$$\sum_{j=a,b,c} i_{sj} = 0 \tag{3.3}$$

In order to adjust the amount of reactive power injected by the compensator into the PCC, a certain pre-defined power factor needs to be maintained at the source, which

implies satisfaction of the following condition [20],

$$\angle\overline{v}_{sa+} = \angle\overline{i}_{sa+} + \psi_+ \tag{3.4}$$

where ψ_+ is the desired angle between $\overline{v}_{sa+}$ and $\overline{i}_{sa+}$.

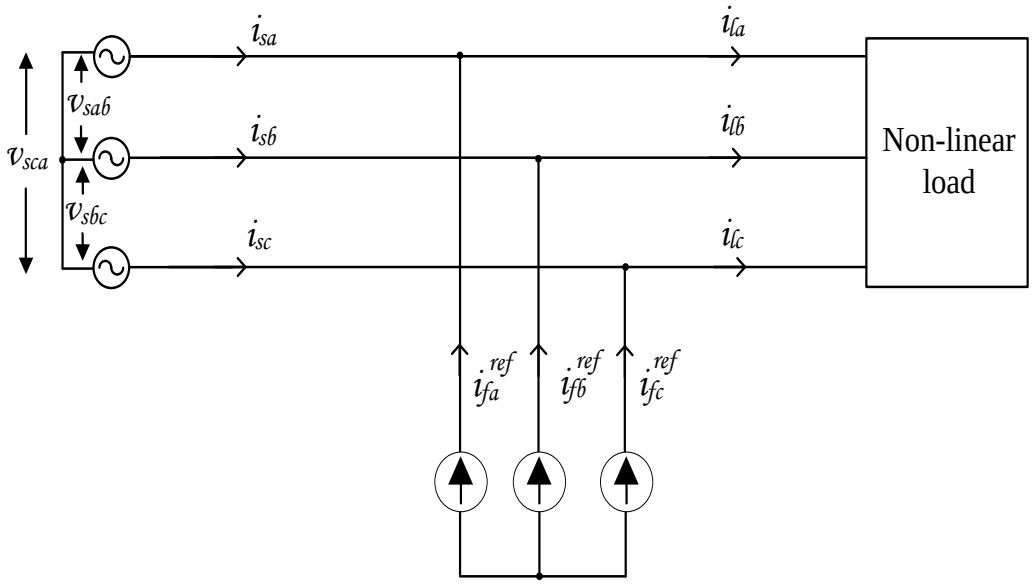

Fig. 3.2: Three phase three wire filter configuration

(3.4) can be rewritten as follows:-

$$\angle(\frac{1}{3} \times [v_{sa} + av_{sb} + a^2 v_{sc}]) = \angle(\frac{1}{3} \times [i_{sa} + ai_{sb} + a^2 i_{sc}]) + \psi_+ \tag{3.5}$$

$$L.H.S = R.H.S \tag{3.6}$$

L.H.S of the above equation can be expressed as below:

$$L.H.S = \angle(\frac{1}{3} \times [v_{sa} + (-\frac{1}{2} + j\frac{\sqrt{3}}{2})v_{sb} + (-\frac{1}{2} - j\frac{\sqrt{3}}{2})v_{sc}]) \tag{3.7}$$

The above equation can be rewritten as

$$L.H.S = \tan^{-1}[\frac{(\frac{\sqrt{3}}{2}) \times (v_{sb} - v_{sc}))}{v_{sa} - v_{sb}/2 - v_{sc}/2}] \tag{3.8}$$

In a similar way R.H.S can be expressed as follows:

$$R.H.S = \angle(\frac{1}{3} \times [i_{sa} + (-\frac{1}{2} + j\frac{\sqrt{3}}{2})i_{sb} + (-\frac{1}{2} - j\frac{\sqrt{3}}{2})i_{sc}]) + \psi_{+} \tag{3.9}$$

The above equation can be rewritten as follows:

$$R.H.S = \tan^{-1}[\frac{(\frac{\sqrt{3}}{2}) \times (i_{sb} - i_{sc}))}{i_{sa} - i_{sb}/2 - i_{sc}/2}] + \psi_{+} \tag{3.10}$$

Taking tangent on both sides and equating ans rearranging, the following expression is obtained:

$$\begin{aligned} \frac{\sqrt{3}}{2} \times (v_{sb} - v_{sc}) \times (i_{sa} - i_{sb}/2 - i_{sc}/2) - \frac{3}{4} \times (v_{sb} - v_{sc}) \times (i_{sb} - i_{sc}) \times \tan(\psi_{+}) \\ - \frac{\sqrt{3}}{2} \times (v_{sa} - v_{sb}/2 - v_{sc}/2) \times (i_{sb} - i_{sc}) \\ - (v_{sa} - v_{sb}/2 - v_{sc}/2) \times (i_{sa} - i_{sb}/2 - i_{sc}/2) \times \tan(\psi_{+}) = 0 \end{aligned} \tag{3.11}$$

The above equation can be rearranged with terms as coefficients of $i_{sj}\ \forall j = a, b, c$. Further we divide the equation by $\frac{\sqrt{3}}{2}$ throughout. Thus, we obtain the following equation.

$$\begin{aligned} \{(v_{sb} - v_{sc}) + \beta \times (v_{sb} + v_{sc} - 2 \times v_{sa})\} i_{sa}^{ref} \\ + \{(v_{sc} - v_{sa}) + \beta \times (v_{sc} + v_{sa} - 2 \times v_{sb})\} i_{sb}^{ref} \\ + \{(v_{sa} - v_{sb}) + \beta \times (v_{sa} + v_{sb} - 2 \times v_{sc})\} i_{sc}^{ref} = 0 \end{aligned} \tag{3.12}$$

where, $\beta = \frac{\tan\psi+}{\sqrt{3}}$, is an indicator of the amount of pre-defined reactive power compensation required and currents $i_{sj}\ \forall j = a, b, c$ are considered as reference currents.

Since, in general, the system under consideration has generators and loads connected in floating neutral configuration, it is advisable to undertake line voltage measurements and not phase voltage measurements. Hence, its ideal to represent (3.12) in

terms of line voltages. Therefore, (3.12) can be simplified as follows:

$$\{(v_{sb}-v_{sc})+\beta\times(v_{sb}+v_{sc}-v_{sa}-v_{sa})\}i_{sa}^{ref} + \{(v_{sc}-v_{sa})+\beta\times(v_{sc}+v_{sa}-v_{sb}-v_{sb})\}i_{sb}^{ref} + \{(v_{sa}-v_{sb})+\beta\times(v_{sa}+v_{sb}-v_{sc}-v_{sc})\}i_{sc}^{ref}=0 \quad (3.13)$$

In the above equation, $v_{sc}-v_{sa}$= v_{sca}. Similarly, $v_{sa}-v_{sb}$= v_{sab} and $v_{sb}-v_{sc}$= v_{sbc}. Therefore, if we represent with the above notations we get the final expression in terms of line voltages as follows:-

$$\{v_{sbc}+\beta\times(v_{sca}-v_{sab})\}i_{sa}^{ref} + \{v_{sca}+\beta\times(v_{sab}-v_{sbc})\}i_{sb}^{ref} + \{v_{sab}+\beta\times(v_{sbc}-v_{sca})\}i_{sc}^{ref}=0 \quad (3.14)$$

Similarly, post compensation, the average load power, P_{lavg}, is assumed to be fed from the source and compensator plays no part in supplying any real component of power. Hence, the following equation holds true for balanced set of voltages and currents [20].

$$\sum_{j=a,b,c} v_{sj}i_{sj}=P_{lavj} \quad (3.15)$$

(3.3), (3.14) and (3.15), expressed as coefficients of i_{sj}, can be written in matrix form as follows.

$$\begin{bmatrix} 1 & 1 & 1 \\ v_{sbc}+\beta(v_{sca}-v_{sab}) & v_{sca}+\beta(v_{sab}-v_{sbc}) & v_{sab}+\beta(v_{sbc}-v_{sca}) \\ v_{sa} & v_{sb} & v_{sc} \end{bmatrix} \begin{bmatrix} i_{sa}^{ref} \\ i_{sb}^{ref} \\ i_{sc}^{ref} \end{bmatrix} = \begin{bmatrix} 0 \\ 0 \\ P_{lavg} \end{bmatrix} \quad (3.16)$$

The objective is to compute reference source currents from the measured source voltage

values. The above equation can be represented in terms of source current values as,

$$\begin{bmatrix} i_{sa}^{ref} \\ i_{sb}^{ref} \\ i_{sc}^{ref} \end{bmatrix} = \begin{bmatrix} v \end{bmatrix}^{-1} \begin{bmatrix} 0 \\ 0 \\ P_{lavg} \end{bmatrix}$$

$$\begin{bmatrix} i_{sa}^{ref} \\ i_{sb}^{ref} \\ i_{sc}^{ref} \end{bmatrix} = \frac{1}{\Delta_v} \begin{bmatrix} v_{11} & v_{12} & v_{13} \\ v_{21} & v_{22} & v_{23} \\ v_{31} & v_{32} & v_{33} \end{bmatrix} \begin{bmatrix} 0 \\ 0 \\ P_{lavg} \end{bmatrix} \tag{3.17}$$

In the above equation, as the first two rows of P column matrix are zeros, only the third column elements have significance in computation, i.e.,

$$\begin{bmatrix} i_{sa}^{ref} \\ i_{sb}^{ref} \\ i_{sc}^{ref} \end{bmatrix} = \frac{1}{\Delta_v} \begin{bmatrix} v_{13} \\ v_{23} \\ v_{33} \end{bmatrix} \begin{bmatrix} P_{lavg} \end{bmatrix} \tag{3.18}$$

The determinant Δ_v can be computed from the v matrix as,

$$\begin{aligned} \Delta_v = \{v_{sca} + \beta \times (v_{sab} - v_{sbc})\}v_{sc} - \{v_{sab} + \beta \times (v_{sbc} - v_{sca})\}v_{sb} - \\ \{v_{sbc} + \beta \times (v_{sca} - v_{sab})\}v_{sc} + \{v_{sab} + \beta \times (v_{sbc} - v_{sca})\}v_{sa} + \\ \{v_{sbc} + \beta \times (v_{sca} - v_{sab})\}v_{sb} - \{v_{sca} + \beta \times (v_{sab} - v_{sbc})\}v_{sa} \end{aligned}$$

$$\begin{aligned} \Delta_v = v_{sca}v_{sc} - v_{sab}v_{sb} - v_{sbc}v_{sc} + v_{sab}v_{sa} + v_{sbc}v_{sb} - v_{sca}v_{sa} + \\ \beta \times (v_{sab}v_{sc} - v_{sbc}v_{sc} - v_{sbc}v_{sb} + v_{sca}v_{sb} - v_{sca}v_{sc} + v_{sab}v_{sc} + \\ v_{sbc}v_{sa} - v_{sca}v_{sa} + v_{sca}v_{sb} - v_{sab}v_{sb} - v_{sab}v_{sa} + v_{sbc}v_{sa}) \end{aligned}$$

$$\begin{aligned} \Delta_v = v_{sab}^2 + v_{sbc}^2 + v_{sca}^2 + \beta \times (2v_{sab}v_s - v_{sbc}v_{sc} - v_{sbc}v_{sb} + 2v_{sca}v_{sb} - v_{sca}v_{sc} + \\ 2v_{sbc}v_{sa} - v_{sca}v_{sa} - v_{sab}v_{sb} - v_{sab}v_{sa}) \end{aligned}$$

$$\Delta_v = v_{sab}^2 + v_{sbc}^2 + v_{sca}^2 + \beta \times \{v_{sab}(v_{sca} - v_{sbc}) - v_{sca}(v_{sab} - v_{sbc}) - v_{sbc}(v_{sca} - v_{sab})\}$$

$$\Delta_v = v_{sab}^2 + v_{sbc}^2 + v_{sca}^2 + \beta \times \{v_{sab}(v_{sca} - v_{sbc}) - v_{sca}(v_{sab} - v_{sbc}) - v_{sbc}(v_{sca} - v_{sab})\}$$

Therefore, the determinant Δ_v is given by,

$$\Delta_v = v_{sab}^2 + v_{sbc}^2 + v_{sca}^2 \tag{3.19}$$

The elements of the v matrix in (3.19) can be computed as follows,

$$v_{13} = -v_{sca} - \beta \times (v_{sab} - v_{sbc}) + v_{sab} + \beta \times (v_{sbc} - v_{sca})$$

$$v_{13} = v_{sab} - v_{sca} + 3\beta \times v_{sbc} \tag{3.20}$$

Also,

$$v_{23} = -v_{sab} - \beta \times (v_{sbc} - v_{sca}) + v_{sbc} + \beta \times (v_{sca} - v_{sab})$$

$$v_{23} = v_{sbc} - v_{sab} + 3\beta \times v_{sca} \tag{3.21}$$

Similarly,

$$v_{33} = v_{sca} + \beta \times (v_{sab} - v_{sbc}) - v_{sbc} - \beta \times (v_{sca} - v_{sab})$$

$$v_{33} = v_{sca} - v_{sbc} + 3\beta \times v_{sab} \tag{3.22}$$

Substituting the values of (3.19), (3.20), (3.21) and (3.22) in (3.18), the following values for source current is obtained,

$$\begin{bmatrix} i_{sa}^{ref} \\ i_{sb}^{ref} \\ i_{sc}^{ref} \end{bmatrix} = \left(\frac{P_{lavg}}{v_{sab}^2 + v_{sbc}^2 + v_{sca}^2} \right) \begin{bmatrix} v_{sab} - v_{sca} + 3\beta \times v_{sbc} \\ v_{sbc} - v_{sab} + 3\beta \times v_{sca} \\ v_{sca} - v_{sbc} + 3\beta \times v_{sab} \end{bmatrix} \tag{3.23}$$

If the system demands 100% reactive power compensation by the filter, so that no reactive power is generated by the source, the value of β in the above equation becomes

zero. Thus (3.23) can be re-formulated as,

$$\begin{bmatrix} i_{sa}^{ref} \\ i_{sb}^{ref} \\ i_{sc}^{ref} \end{bmatrix} = \left(\frac{P_{lavg}}{v_{sab}^2 + v_{sbc}^2 + v_{sca}^2} \right) \begin{bmatrix} v_{sab} - v_{sca} \\ v_{sbc} - v_{sab} \\ v_{sca} - v_{sbc} \end{bmatrix} \tag{3.24}$$

In the above equation, v_{sab}, v_{sbc} and v_{sca} are the measured source line voltages at the switchboard terminal. The source currents computed in (3.24) are the instantaneous currents generated by the source in each phase to meet a purely resistive load of P_{lavg} rating i.e. the source sees the load as a purely resistive load with no source reactive power generation. Furthermore, because the filter works as a regulated source for harmonic currents, the compensator will cancel out the harmonics generated by the non-linear load. To achieve source power factor unity, the currents generated in each phase will be in phase with the respective phase voltages.

Full reactive power compensation and pure harmonic cancellation, on the other hand, are only possible if the source provides pure sinusoidal voltage waveforms. This can not be assumed true for a ship based generator as the high source impedance (15-20%) can result in voltage harmonics at the generator output terminal, if the current has significant harmonics present in it. Hence, the fundamental positive sequence components need to be extracted for the measured line voltages and thus, (3.24) needs to be modified by replacing the measured line voltages with its corresponding fundamental positive sequence line voltage values for error-free calculation of reference source currents [23]. This will be covered in the subsequent section.

3.2.2 Generation of Fundamental Positive Sequence Components

The positive sequence component can be extracted from the instantaneous 3 phase voltage waveform using (3.1). Consider the following balanced distorted 3 phase line voltage waveforms,

$$v_{ab} = V_{dc} + V_{lm1} sin(\omega t + \phi_1) + V_{lm2} sin(2\omega t + \phi_2) + ...$$

$$v_{bc} = V_{dc} + V_{lm1}sin(\omega t - 120^\circ + \phi_1) + V_{lm2}sin(2(\omega t - 120^\circ) + \phi_2) + ...$$

$$v_{ca} = V_{dc} + V_{lm1}sin(\omega t + 120^\circ + \phi_1) + V_{lm2}sin(2(\omega t + 120^\circ) + \phi_2) + ... \quad (3.25)$$

The positive sequence component of the three phase voltages given in (3.25) is given by,

$$\overline{v}_{ab+} = \frac{1}{3}(v_{ab} + av_{bc} + a^2v_{ca}) \quad (3.26)$$

After evaluating the positive sequence component of $\overline{v}_{ab+}$, the positive sequence component of the other two line voltages can be evaluated as,

$$\overline{v}_{bc+} = a^2\overline{v}_{ab+} \quad (3.27)$$

And,

$$\overline{v}_{ca+} = a\overline{v}_{ab+} \quad (3.28)$$

The fundamental component of the voltages given in (3.26), (3.27) and (3.28) can be extracted using the following equations [20].

$$\overline{V}^f_{ab+} = \frac{\sqrt{2}}{T}\int_{t1-T}^{T} \overline{v}_{ab+}(t)e^{-j(\omega t - \frac{\pi}{2})}dt \quad (3.29)$$

Similarly,

$$\overline{V}^f_{bc+} = \frac{\sqrt{2}}{T}\int_{t1-T}^{T} \overline{v}_{bc+}(t)e^{-j(\omega t - \frac{\pi}{2})}dt \quad (3.30)$$

and,

$$\overline{V}^f_{ca+} = \frac{\sqrt{2}}{T}\int_{t1-T}^{T} \overline{v}_{ca+}(t)e^{-j(\omega t - \frac{\pi}{2})}dt \quad (3.31)$$

After computing the values of $\overline{V}^f_{ab+}$, $\overline{V}^f_{bc+}$ and $\overline{V}^f_{ca+}$, the respective time varying quantities can be expressed as,

$$v^f_{ab+}(t) = \sqrt{2}|\overline{V}^f_{ab+}|\sin(wt + \angle\overline{V}^f_{ab+}) \quad (3.32)$$

$$v^f_{bc+}(t) = \sqrt{2}|\overline{V}^f_{bc+}|\sin(wt + \angle\overline{V}^f_{bc+}) \quad (3.33)$$

$$v^f_{ca+}(t) = \sqrt{2}|\overline{V}^f_{ca+}|\sin(wt + \angle\overline{V}^f_{ca+}) \quad (3.34)$$

After extracting the fundamental positive sequence time varying components of voltages v_{ab}, v_{bc} and v_{ca}, (3.23) can be modified as,

$$\begin{bmatrix} i_{sa}^{ref} \\ i_{sb}^{ref} \\ i_{sc}^{ref} \end{bmatrix} = \left(\frac{P_{lavg}}{{v_{sab+}^{f}}^2 + {v_{sbc+}^{f}}^2 + {v_{sca+}^{f}}^2} \right) \begin{bmatrix} v_{sab+}^{f} - v_{sca+}^{f} + 3\beta \times v_{sbc+}^{f} \\ v_{sbc+}^{f} - v_{sab+}^{f} + 3\beta \times v_{sca+}^{f} \\ v_{sca+}^{f} - v_{sbc+}^{f} + 3\beta \times v_{sab+}^{f} \end{bmatrix} \tag{3.35}$$

The reference source currents generated according to (3.35) will result in ideal compensation with harmonic cancellation and pre-defined reactive power compensation.

3.3 Computation of Average Load Power, P_{lavg}

A proper computation of average load power, which can be performed by averaging the instantaneous power across a complete cycle, is required to achieve error-free compensation, i.e.,

$$P_{lavg} = \frac{1}{T} \int_{t1}^{t1+T} (v_{sa} i_{la} + v_{sb} i_{lb} + v_{sc} i_{lc}) dt \tag{3.36}$$

When the voltage incorporates harmonics, however, the above equation is prone to errors and may result in changing values of average load power. Furthermore, because the measurement is for line voltages, calculating v_a, v_b and v_c is tricky. P_{lavg} can also be calculated using the fundamental positive sequence components of voltage and current, as shown in the equation below.

$$P_{lavg} = \sqrt{3} |\overline{V}_{ab+}^{f}| |\overline{I}_{a+}^{f}| \cos\psi + \tag{3.37}$$

In the above equation, $\overline{V}_{ab+}^{f}$ is computed in (3.29). Similarly, the fundamental positive sequence component of line current can also be computed, which is given by

$$\overline{I}_{a+}^{f} = \frac{\sqrt{2}}{T} \int_{t1-T}^{T} \bar{i}_{a+}(t) e^{-j(\omega t - \frac{\pi}{2})} dt \tag{3.38}$$

where,

$$\bar{i}_{a+} = \frac{1}{3}(i_a + a i_b + a^2 i_c)$$

Because the values of voltage and current post compensation match their respective basic values, the (3.37) offers a relatively accurate figure of average load power. The fundamental power factor will be unity after compensating for 100% reactive power compensation. As a result, omitting the power factor component from the average load power calculation is acceptable.

3.4 Compensator Power Loss Calculation, P_{loss}

For harmonic current and reactive power generation, the active power filter is essentially an inverter with a DC link capacitor at its input. Because it generates no active power, the voltage of an ideal DC link capacitor should remain constant. A practical system, on the other hand, takes into account switching and other losses in the inverter. This will eventually result in a drop in DC link voltage, which may result in incorrect compensation. A PI controller is used to maintain the DC link voltage at the given reference value, and the losses in the compensator are fed from the source. A conventional PI controller for maintaining DC link voltage is expressed as,

$$P_{loss} = k_p e_{dc} + k_i \int e_{dc} dt \tag{3.39}$$

where, k_p and k_i are the proportional and integral gains of the PID controller and e_{dc} is the error signal, which is the difference between a pre-defined reference voltage value and the actual DC link voltage value i.e.,

$$e_{dc} = V_{ref} - V_{dc}$$

The above mentioned power based conventional design has a problem, according to Mahesh Kumar et al. [28], in that its transient reaction is slow and the design is rather challenging for a complicated system. The authors suggest an energy-based fast-acting DC link voltage controller to address these shortcomings. The energy necessary to shift

the dc link voltage from V_{dc} to V_{ref} in this design is given by the following equation:

$$W = \frac{1}{2} C_{dc}[V_{ref}^2 - V_{dc}^2] \tag{3.40}$$

where, C_{dc} is the capacitance of the DC link capacitor. If the ripple frequency is given by f_r, then the power associated with the energy term given in (3.40) is given by,

$$P_{loss}^{mod} = \frac{1}{2} f_r C_{dc}[V_{ref}^2 - V_{dc}^2] \tag{3.41}$$

The aforementioned equation can be used to modify the conventional controller in (3.39) to define a new controller with varied proportional and integral gains to achieve a fast-acting controller with improved transient responsiveness. As a result, the modified equation for a fast-acting controller is as follows:

$$P_{loss}^{mod} = k_p^{'} e_{dc}^{'} + k_i^{'} \int e_{dc}^{'} dt \tag{3.42}$$

where, $k_p^{'}$ and $k_i^{'}$ are the modified proportional and integral gains of the PID controller and $e_{dc}^{'}$ is the modified error signal, which is given by,

$$e_{dc}^{'} = V_{ref}^2 - V_{dc}^2$$

Figures 3.3 and 3.4 show the generation of power loss using a conventional controller

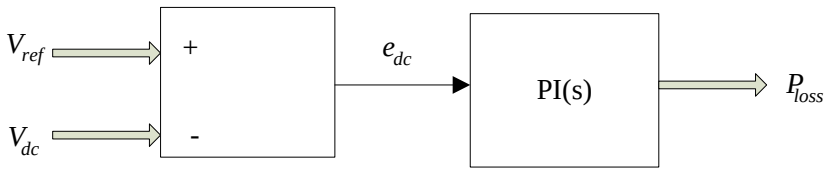

Fig. 3.3: Conventional PI controller for P_{loss} generation

and a fast-acting controller, respectively. One of the most significant benefits of employing a fast acting controller is the ease with which proportional and integral gains may be calculated. The value of proportionate gain can be calculated by comparing

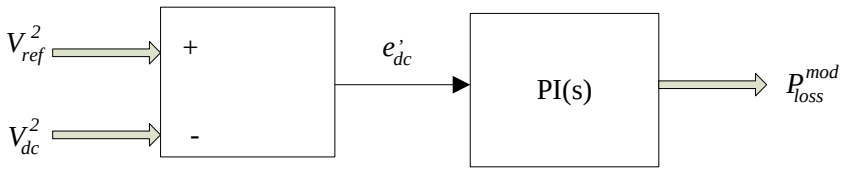

Fig. 3.4: Fast-Acting PI controller for P_{loss}^{mod} generation

(3.41) and (3.42).

$$k_p^{'} = \frac{f_r C_{dc}}{2} \tag{3.43}$$

Once the value of $k_p^{'}$ is determined, the value of integral gain can be easily computed. The value of $k_i^{'}$ is chosen as a trade-off between the amount of overshoot in compensated source currents and better transient response. For an ideal compensator with good transient response and limited overshoot, the value of $k_i^{'}$ is chosen as half the value of $k_p^{'}$ [28], i.e.,

$$k_i^{'} = \frac{k_p^{'}}{2} \tag{3.44}$$

3.5 Reference Filter Currents Calculation

The load currents, i_{La}, i_{Lb} and i_{Lc}, are measured at the input side of the load prior to the rectifier and since the filter is responsible for injecting harmonic currents required for the load, the following is obtained after application of Kirchoff's current law at the input side of the filter,

$$\begin{bmatrix} i_{fa}^{ref} \\ i_{fb}^{ref} \\ i_{fc}^{ref} \end{bmatrix} = \begin{bmatrix} i_{La} \\ i_{Lb} \\ i_{Lc} \end{bmatrix} - \begin{bmatrix} i_{sa}^{ref} \\ i_{sb}^{ref} \\ i_{sc}^{ref} \end{bmatrix} \tag{3.45}$$

Substituting the values of i_s^{ref} matrix computed in (3.35) in the above equation, reference filter currents can be computed as,

$$\begin{bmatrix} i_{fa}^{ref} \\ i_{fb}^{ref} \\ i_{fc}^{ref} \end{bmatrix} = \begin{bmatrix} i_{La} \\ i_{Lb} \\ i_{Lc} \end{bmatrix} - \left(\frac{P_{lavg}}{{v_{sab+}^f}^2 + {v_{sbc+}^f}^2 + {v_{sca+}^f}^2} \right) \begin{bmatrix} v_{sab+}^f - v_{sca+}^f + 3\beta \times v_{sbc+}^f \\ v_{sbc+}^f - v_{sab+}^f + 3\beta \times v_{sca+}^f \\ v_{sca+}^f - v_{sbc+}^f + 3\beta \times v_{sab+}^f \end{bmatrix} \tag{3.46}$$

The loss component of the compensator should be fed from the source, as indicated in the preceding section, to avoid DC link voltage collapse. The P_{loss} component should therefore be routed through the desired reference source currents. This ensures that the DC connection voltage remains constant or close to it. As a result, filter reference currents are expressed as,

$$\begin{bmatrix} i_{fa}^{ref} \\ i_{fb}^{ref} \\ i_{fc}^{ref} \end{bmatrix} = \begin{bmatrix} i_{La} \\ i_{Lb} \\ i_{Lc} \end{bmatrix} - \left(\frac{P_{lavg} + P_{loss}}{{v_{sab+}^f}^2 + {v_{sbc+}^f}^2 + {v_{sca+}^f}^2} \right) \begin{bmatrix} v_{sab+}^f - v_{sca+}^f + 3\beta \times v_{sbc+}^f \\ v_{sbc+}^f - v_{sab+}^f + 3\beta \times v_{sca+}^f \\ v_{sca+}^f - v_{sbc+}^f + 3\beta \times v_{sab+}^f \end{bmatrix} \tag{3.47}$$

For unity power factor operation $(\beta = 0)$, (3.47) can be modified as,

$$\begin{bmatrix} i_{fa}^{ref} \\ i_{fb}^{ref} \\ i_{fc}^{ref} \end{bmatrix} = \begin{bmatrix} i_{La} \\ i_{Lb} \\ i_{Lc} \end{bmatrix} - \left(\frac{P_{lavg} + P_{loss}}{{v_{sab+}^f}^2 + {v_{sbc+}^f}^2 + {v_{sca+}^f}^2} \right) \begin{bmatrix} v_{sab+}^f - v_{sca+}^f \\ v_{sbc+}^f - v_{sab+}^f \\ v_{sca+}^f - v_{sbc+}^f \end{bmatrix} \tag{3.48}$$

The preceding mathematical formulation for filter reference current generation necessitates an effective inverter management approach so that the reference currents can be generated using the inverter module's DC link capacitor. This necessitates a strong control strategy, which will be covered in the next section.

3.6 Methodology for Inverter Control

Despite the abundance of control strategies available in the literature, the hysteresis band current control method is widely accepted for generation of control signals for inverters used in active filters because of its quick controllability, ease of implementation, and insensitivity to load parameter variations [30]. The control signals for the inverter switches are created in this technique, resulting in an output current waveform that follows a reference current waveform. The implementation of a hysteresis band current controller is shown in Fig. 3.5.

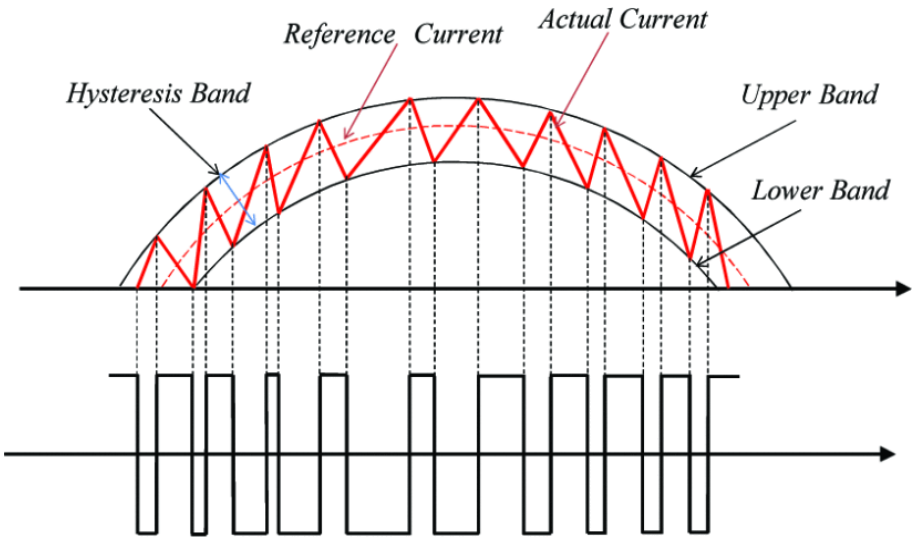

Fig. 3.5: Implementation of hysteresis band current controller [31]

Because the inverter switches are controlled asynchronously, the switching frequency cannot be precisely specified, which is a well-known shortcoming of the hysteresis band current control method. Furthermore, a lack of coordination between the controllers of the various phases might result in a high switching frequency, which increases the inverter's switching losses. The DC link capacitor voltage will collapse as a result of this. However, by properly designing the values of the hysteresis band and coupling inductor [29]-[30], the switching frequency may be limited.

The algorithm used for implementation of hysteresis band current control method for generation of control signals for the inverter switches is explained below.

If (i_{fa} - i_{fa}^{ref}) $\leq h$, then the upper leg switch of phase-a is turned on and lower leg

switch of phase-*a* is turned off i.e. S_A = 1 and $\overline{S}_A$ = 0.

Else if, (i_{fa} - i_{fa}^{ref}) $\geq h$, then the upper leg switch of phase-*a* is turned off and lower leg switch of phase-*a* is turned on i.e. S_A = 0 and $\overline{S}_A$ = 1.

Else if, (i_{fa}^{ref} - h) $< i_{fa} <$ (i_{fa}^{ref} + h), then retain the current status of the switches in phase-*a* leg.

where, i_{fa} is the actual filter current in phase-*a*, h is the hysteresis band, (i_{fa}^{ref} - h) and (i_{fa}^{ref} + h) forms the lower and upper bands of reference filter current of phase-*a*.

Similar algorithm is extended for phase-*b* and phase-*c* as,

If (i_{fb} - i_{fb}^{ref}) $\leq h$, S_B = 1 and $\overline{S}_B$ = 0.

Else if, (i_{fb} - i_{fb}^{ref}) $\geq h$,S_B = 0 and $\overline{S}_B$ = 1.

Else if, (i_{fb}^{ref} - h) $< i_{fb} <$ (i_{fb}^{ref} + h), then retain the current status of the switches in phase-*b* leg.

and,

If (i_{fc} - i_{fc}^{ref}) $\leq h$, S_C = 1 and $\overline{S}_C$ = 0.

Else if, (i_{fc} - i_{fc}^{ref}) $\geq h$,S_C = 0 and $\overline{S}_C$ = 1.

Else if, (i_{fc}^{ref} - h) $< i_{fc} <$ (i_{fc}^{ref} + h), then retain the current status of the switches in phase-*c* leg.

The above algorithm clearly shows that, despite the lack of coordination between the *a*, *b*, and *c* phases, the implementation of the above logic is simpler than alternative control strategies, making the method commonly accepted for following reference currents in active power filters.

3.7 Interfacing Passive Filter and Shunt Capacitance

An ordinary interfacing inductor is the most widely used component for smoothing the output currents from a VSI [27], however, it suffers from the disadvantages of bulky

design, which results in more voltage drop across the filter. Additionally, the harmonic attenuation of L filter is not very pronounced [36], which makes an LCL filter the next viable option as an interfacing filter. However, in the proposed configuration we are interfacing a passive filter in series with the active filter to make it function as a hybrid filter. A hybrid filter configuration is shown in Fig. 3.6. This configuration helps in reducing DC link voltage of the VSI [37]. Additionally, a shunt capacitance is also added which aids in largely eliminating the switching frequency components of the VSI in the terminal voltages and source currents.The injection of higher order switching frequency ripples and the effect of EMI can cause damaging effects on warships as multiple radar/ weapon sensors and communication equipment works at higher frequencies. Fig. 3.6

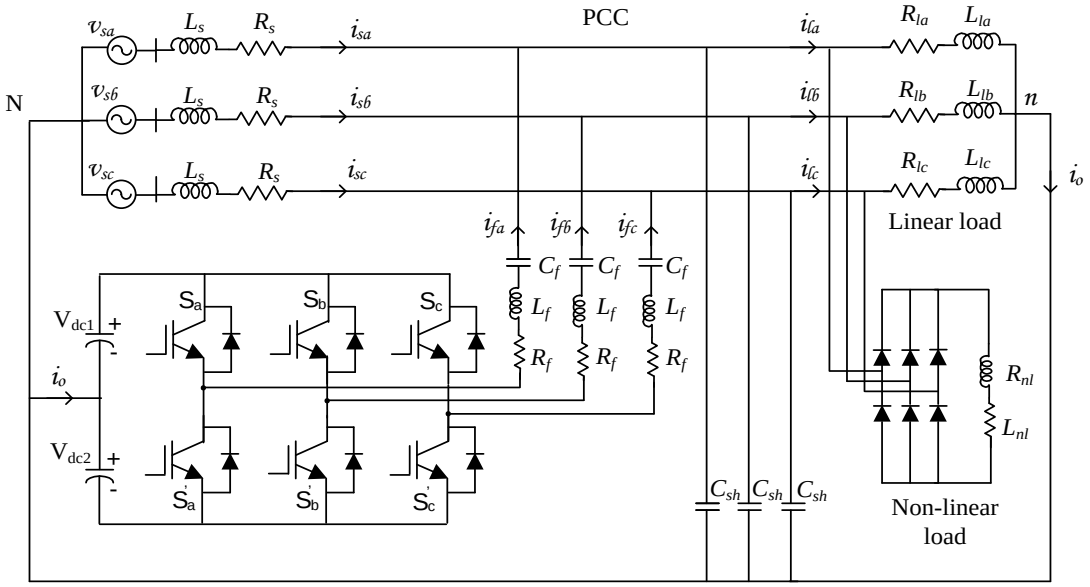

Fig. 3.6: DSTATCOM with interfacing passive filter

shows the equivalent circuit of a neutral clamped VSI topology-based DSTATCOM. It is a combination of the conventional DSTATCOM topology with a capacitor C_f in series with the interfacing shunt branch of the active filter and a capacitor C_{sh} in shunt with the active filter. This topology is referred to as hybrid topology. The passive capacitor C_f has the capability to supply a part of the reactive power required by the load, and the active filter will compensate the balance reactive power and the harmonics present in the load. The addition of capacitor in series with the interfacing inductor of the conventional topology will significantly reduce the dc-link voltage requirement and consequently reduces the average switching frequency of the switches. This is be-

cause, when the load is inductive in nature, the fundamental of the filter current lags the voltage at the PCC by 90 degrees for reactive power compensation, and thus, the fundamental voltage across the capacitor again lags the fundamental filter current by 90 degrees. Finally, the fundamental voltage across the capacitor will be in phase opposition to the voltage at the PCC. Thus, the fundamental voltage across the capacitor adds to the inverter terminal voltage. This allows us to rate the dc-link voltage at lower value than conventional design. The designer may choose the value of dc-link voltage to be reduced, such that the LC filter in the active filter leg of each phase offers minimum impedance to the fundamental frequency component and higher impedance for switching frequency components [37].

Additionally, the reduction in average switching frequency with the proposed topology can be explained as follows. As the voltage across the inductor is high in case of the conventional topology, the rate of rise of filter current di_f /dt will be higher than that of the proposed topology. This will allow the filter current to hit the hysteresis boundaries at a faster rate and increases the switching, whereas in proposed hybrid topology, the number of switchings will be less. Thus, the average switching frequency of the switches in the proposed topology will be less as compared to the conventional topology. Since the average switching is less, the switching loss will also decrease in the proposed topology. One more advantage of having less voltage across the inductor is that the hysteresis band violation will be less. This will improve the quality of compensation and total harmonic distortion (THD) will be less in the proposed topology [37].

A slightly differently explained version of the hybrid filter was also learned from literature. L. Wang et al. [38] explains the selection of series capacitance and shunt capacitance in a hybrid filter in a different way. The paper in fact uses a Static VAR compensator in place of shunt capacitor. However, it is understood that the function of the Static VAR compensator is same as that of a shunt capacitor. The circuit configuration of a three phase three wire Static VAR compensator in parallel with a hybrid active filter is shown in Fig. 3.7.

Here the Static VAR compensator part consists of a coupling inductor L_c, a parallel

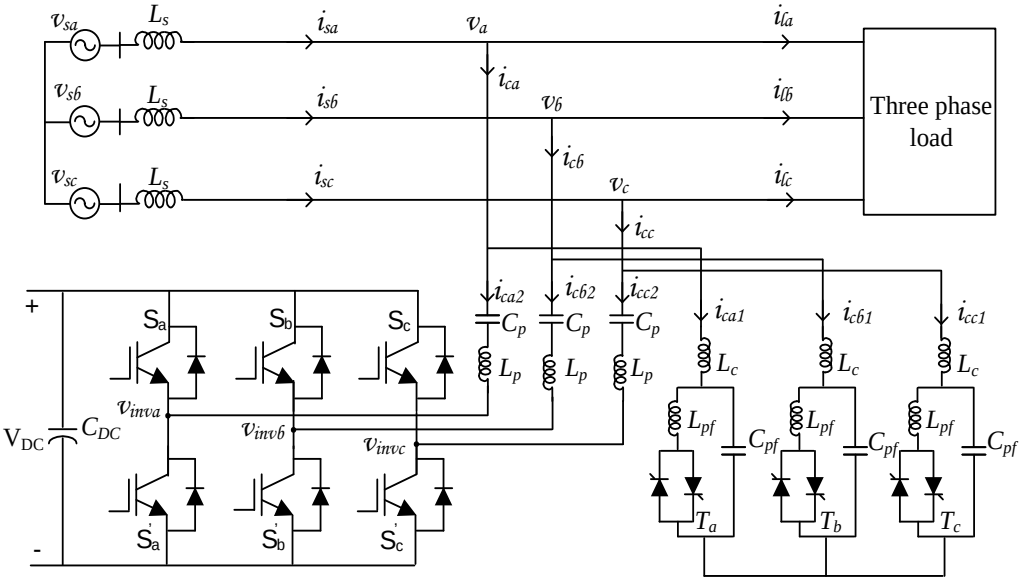

Fig. 3.7: Static VAR compensator in parallel with a hybrid active filter

capacitor C_{pf} and a Thyristor controller reactor with an inductor L_{pf}. The Hybrid active power filter part consists of a coupling LC filter with L_p and C_p as the inductance and capacitance respectively. Here the VSI part has both low voltage rating due to coupling LC filter and low current rating due to Static VAR compensator. The coupling LC filter is used to compensate a fixed amount of reactive power at the fundamental frequency, while the Static VAR compensator part impedance is used to dynamically compensate the reactive power difference between the LC filter and the loads by controlling its firing angle. Further, literature explains the purpose of L_P here as to provide a low LC impedance at the most dominated harmonic order, so that the required DC link voltage for harmonic compensation can be reduced. Design of C_{pf} and C_p are undertaken in such a way that together they will contribute to reactive power compensation. The purpose of design of L_c is to filter the harmonic currents generator due to thyristor switching. The configuration above is very much similar to our proposed topology, however designing aspects are different. Literature [38] suggests that the usage of the above topology can reduce the cost of filter drastically. Hence, the same can be considered as future scope of this project.

Though the current topology does not use an LCL filter, the following is known about an LCL filter from literature. Both the inverter and grid side inductors in an

LCL filter are intended to decrease current ripples at switching frequency, while the capacitor rating is determined by the proportion of fundamental reactive power that must be supplied by the capacitor [35]. A resistor is also connected in series with the capacitor to provide passive damping and prevent resonance. However, in order to limit power loss in the components, the resistance is kept low. Marco Liserre et al. 33] suggested that the main criterion for selecting the values of components in LCL filter is to limit the installed reactive element size, so as to achieve better power factor and to reduce filter power losses. Sampath Jayalath et al. [32] defined the following characteristic requirements for a well designed filter.

- less voltage drop across filter elements
- less reactive power by filter capacitor
- good power factor operation
- less stored energy in the filter elements
- good damping to resonance with reduced damping losses
- low electromagnetic interference

(a) **Value of Shunt Capacitance** C_{sh}

The terminal voltages are distorted due to imbalance and nonlinear load currents in the presence of source impedance, i.e., a nonstiff source in the system. As a result, these voltages cannot be used to generate reference quantities. Positive-sequence voltages at the terminal are extracted using the power-invariant instantaneous symmetrical transformation and used to generate reference currents to improve performance [37]. However, the inverter switching frequency components have contaminated the terminal voltages. These switching frequency components can be removed by adding a filter capacitor C_{sh} in shunt at the PCC in each phase, as shown in Fig. 3.6. While designing the shunt capacitor, it should be ensured that the source reactance L_s and the shunt capacitor C_{sh} do not resonate at the fundamental frequency. If the filter capacitor resonate with the feeder reactance at a frequency ω_r then we get

$$C_{sh} = \frac{1}{{\omega_r}^2 L_s} \tag{3.49}$$

When ω_r is equal to fundamental frequency ω_0 , the aforementioned capacitance is denoted as C_{sh0}. Since resonance between the source reactance and shunt filter capacitor should be avoided at fundamental frequency, C_{sh} should not be chosen near to C_{sh0}. If C_{sh} is very large, the impedance between the PCC and ground becomes very small and results in high filter currents, which will, in turn, increase the source currents, so C_{sh}»C_{sh0} is not valid.

(b) **Value of Interfacing Inductance**

Selection of Interfacing Inductor is the next important step in VSI design. The proper selection of interfacing inductor plays a crucial role in tracking of given reference currents. If the value of interfacing inductance is very large then the value of DC link voltage also should be more to achieve good compensation. The maximum value of switching frequency is considered for designing interfacing inductance. The following expression is used in determining interfacing inductance [21].

$$L_f = \frac{1.6 V_{dc}}{4 f_{swmax} h} \tag{3.50}$$

where, L_f is the inverter side inductance, V_{dc} is the DC link voltage, f_{swmax} is the switching frequency, and h is the hysteresis band. Mahesh Kumar et al. [21] suggests the following design criteria for choosing maximum switching frequency and hysterisis band selection.

The maximum possible switching frequency of the VSI is depending on the type of switches used. To achieve higher switching frequency such as 100kHz, MOSFET switches should be used, but their voltage and current rating are smaller as compared to IGBT switches. However, large value of current cannot be switched at high frequency and lead to electromagnetic interference problem. The IGBT switches are generally preferred due to their higher power handling capacity, good switching speed and low power gating. Typically, maximum frequency of the IGBT switches is around 20 kHz. Similarly, hysterisis band is chosen in such

a way that the percentage THD of the source currents is limited to 5 percent. This can be achieved by keeping hysterisis value as 5-10 percent of the reference compensating currents.

(c) **Value of Series Capacitor**

When calculating the series capacitor value, the fundamental filter current drawn by the shunt filter capacitor is ignored. This is because when C_{sh} is chosen significantly smaller than C_{sh0} at fundamental frequency, the impedance between the PCC and ground becomes very large, and hence the fundamental current drawn by the shunt capacitor is negligible. The C_f's design is determined by how low the dc-link voltage is decreased. Loads with exclusively nonlinear current components are uncommon, and the majority of electrical loads include a combination of linear inductive and nonlinear loads. The proposed hybrid topology will perform well under these situations. To ensure that the planned C_f will work satisfactorily under all other loading situations, the value of C_f is designed at the greatest load current, i.e. with the lowest load impedance. If S_{max} is a system's maximum kVA rating and V_{base} is the system's base voltage, then the system's minimum impedance is [37]

$$Z_{min} = \frac{V_{base}^2}{S_{max}} = mag(R_l + jX_l) \tag{3.51}$$

The shunt filter current must supply the requisite load reactive current in order to attain unity power factor, i.e., the imaginary part of the filter current must match the imaginary portion of the load current. The following are the filter and load currents for each phase [37].

$$I_{filter} = \frac{V_{inv1} - V_{t1}}{R_f + j(X_{lf} - X_{cf})} \tag{3.52}$$

$$I_{load} = \frac{V_{t1}}{R_l + j(X_l)} \tag{3.53}$$

where $\mathrm{X}_{lf} = 2\pi f L_f, X_l = 2\pi f L_l, X_{cf} = \frac{1}{2\pi f L_f}$

and f is the supply frequency of fundamental voltage.

Equating the imaginary parts of the aforementioned equations gives

$$\frac{V_{t1}X_l}{{R_l}^2 + {X_l}^2} = \frac{V_{inv1} - V_{t1}}{(X_{lf} - X_{cf})^2} \times (X_{lf} - X_{cf}) \tag{3.54}$$

where V_{inv1} and V_{t1} are the line to neutral rms voltage of the inverter and the PCC voltage at the fundamental frequency respectively. The fundamental component of inverter voltage in terms of DC link voltage is given as follows:-

$$V_{inv1} = \frac{0.612V_{dc}}{\sqrt{3}} \tag{3.55}$$

Using (3.54) the value of capacitance C_f can be determined.

3.8 Summary

This chapter introduced the concept of instantaneous symmetrical component theory for reference current generation in active load compensation technique using DSTATCOM. The design criteria for undertaking effective inverter control including the DC link capacitor voltage control have been discussed in detail in this chapter. The characteristic requirements of a well designed hybrid filter and computation of filter parameters for smoothing the filter currents have also been presented. Selection of system parameters for undertaking simulations have been explained in detail in next chapter.

CHAPTER 4

SELECTION OF SYSTEM PARAMETERS

4.1 Introduction

As discussed in Chapter 2, the generators and loads used on a marine platform differ slightly from those used on land. The computation of a maritime system's generator and load characteristics is required for a successful simulation. Additionally, for the load and source under consideration, it is necessary to determine the values of compensator parameters that result in pure harmonic cancellation and reactive power compensation. In Chapter 2, many system parameters for design consideration were discussed in depth. These designs have been further developed for a marine platform, which will be discussed in greater detail in the next parts.

4.2 Selection of Generator Parameters

The generator parameters are chosen as per the data obtained from Indian Navy for an upcoming full electric ship which is in proposal stage. The actual generator under consideration would be a 3.3 kV diesel alternator, with short circuit MVA of 50 MVA. However, in this project for proving the system and for simplicity, a prototype model of the same with a reduced rating is considered. Hence, the generator considered in this project has a rating of 230V phase to neutral RMS voltage and power rating of 15 kVA. Further, the per phase generator source reactance is 10 Ω and per phase source resistance is 1 Ω. Thus the X/R ratio is 10. For the said source reactance, the source inductance is computed as 31.8mH.

4.3 Selection of Load Parameters

The load under consideration is a 0.1 MW, 0.85 pf propulsion motor (induction type) fed from a 6-pulse diode front end rectifier-inverter set. However, here since we are using a prototype model, the load is taken as a 1.37 kW, 0.85pf propulsion motor (induction type). It is assumed that the system generates a maximum current harmonics of 30% and demands a maximum reactive power of 0.86 kVAr from the source. In addition, to replicate the actual scenario where the generator is also connected with other loads, here we are connecting few other unbalanced 3 phase loads also with the generator in parallel with the propulsion load. The proposed filter is connected at the input of the rectifier to achieve pure harmonic cancellation and full reactive power compensation.

The various source and load parameters obtained in Sections 4.2 and 4.3 are as shown in Table 4.1 and the same is fed in the simulink generator/ load model.

Table 4.1: Source and load parameters

Parameters	**Values**
Source voltage (Phase to neutral)	230 V
SC level	15 kVA
Source reactance	10 Ω
Source resistance	1 Ω
Source inductance	31.8 mH
Load Active Power	1.37 kW
Load power factor	0.85
Load Reactive Power	0.86 kVAr
Phase *a* other load	34+j47.5 Ω
Phase *b* other load	81+j39.6 Ω
Phase *c* other load	31.5+j70.9 Ω

4.4 Passive Filter Designing

Before undertaking the design of a hybrid filter for the system, an analysis of the performance of the system with a passive filter alone is essential. This will aid in clearly understanding the benefits of a hybrid filter. A passive filter can be designed for har-

monic cancellation as discussed in Chapter 2. These filters are connected in parallel to the non-linear load on the AC side and are adjusted to a specific resonant frequency. It is made up of inductors and capacitors linked to a three-phase line in a star or delta configuration, and it serves as a low-impedance channel for tuned frequency currents. Initially, value of capacitance is selected for compensating reactive power in part or full, which is given in the (2.1)

$$C_f = \frac{1502}{3 \times 2\pi \times 50 \times 230^2} \tag{4.1}$$

Thus we get, C_f = 30.12 μF Assuming the reactive power to be compensated Q_f as 1502 VAR, per phase grid voltage V_g as 230V and supply frequency f_s as 50 Hz we obtain the above.

Once the capacitor is designed, the value of inductance can be computed for a tuned harmonic frqeuency ω_r as given by (2.2). Here fifth harmonic being most prominent, the filter is tuned for compensating fifth harmonic. Thus the value of inductance L_f can be computed as

$$L_f = \frac{1}{(2\pi \times 50 \times 5)^2 \times 30.12 \times 10^{-6}} \tag{4.2}$$

Thus we get, L_f = 0.0135 H. The above computed values of inductance and capacitance can be used for designing passive filter. However, this passive filter is only meant for analysis purpose. Hence the design of actual proposed hybrid filter will be discussed in the following sections.

4.5 DC Link Voltage determination, V_{dc}

Selection of DC link voltage is particularly important for ensuring the stability of DC link capacitor. It should neither be set high nor low to prevent the rise or collapse of DC voltage thereby preventing the destruction of critical circuit elements. Mahesh Kumar et al. [21], proposed a constraint on maintaining the DC link voltage for a single phase

system. The same is extended for a three phase system as,

$$V_{L-pk} \leq V_{dc} \leq V_{CErated} \tag{4.3}$$

where, V_{L-pk} is the peak value of grid line voltage and $V_{CErated}$ is the rated collector emitter voltage of the switches used.

Further S. Karanki et al. [37] suggests that the compensation performance of any active filter depends on the voltage rating of dc-link capacitor. It is proposed that the dc-link voltage should have much higher value than the peak value of the line-to-neutral voltages. This is done in order to ensure a proper compensation at the peak of the source voltage. The authors also discusses the current distortion limit and loss of control limit, which states that the dc-link voltage should be greater than or equal to 6 times the phase voltage of the system for distortion-free compensation. When the dc-link voltage is less than this limit, there is insufficient resultant voltage to drive the currents through the inductances so as to track the reference currents. Due to these criteria, many researchers have used a higher value of dc capacitor voltage based on their applications.

Similarly, Nafih M Ismail et al. [24] has suggested the ideal value of dc link voltage as 1.6 times V_{L-pk} for improved THD and better system performance. If 1.6 times V_{L-pk} is selected, then V_{dc} = 520V.

However, the advantage of the proposed topology is reduction of DC link voltage as brought out by S. Karanki et al. [37]. The present topology consists of two capacitors, one is in series with the interfacing inductor of the active filter and the other is in shunt with the active filter. The series capacitor enables reduction in dc-link voltage while simultaneously compensating the reactive power required by the load, so as to maintain unity power factor without compromising DSTATCOM performance. Hence, the dc link voltage here can be chosen as 300V with the proposed topology.

4.6 Selection of DC Link Capacitance, C_{dc}

The transient response and the duration during which the sag/ swell must be managed are used to determine the DC link capacitance. The capacitance must be well-designed in order for the compensator to manage system performance during transients [22]. The maximum kVA limitations, under transient, which require compensation, must be defined for proper design.

The transient circumstances are not extremely sudden because the speed differences are normally gradual, except for fast attack crafts or speed boats, where the speed variations are quite sharp. Due to the thermal profile restrictions on the diesel engine and the fact that a sudden increase or decrease in motor speed does not have an immediate effect on the actual speed of the ship in water, the variation in speed on a frigate, destroyer, or aircraft carrier is often gradual. Even if the circumstance requires unexpected speed fluctuations or manoeuvring during drills or during a battle, a ship's gas turbine engine with CODLAG configuration will be able to do it. Because electric propulsion is extensively employed during normal travel, the loading and unloading of an electric propulsion ship's diesel engine takes only a few seconds to minutes. In this case, the transients that need to be handled by the compensator is limited only to almost 20-25% of rated kVA of the system, i.e., for designing a compensator for S_p kVA propulsion system, assuming that the energy required to handle transients be S_p and $0.25S_p$ for n cycles, then the change in energy handled by the capacitor is given as [21],

$$\Delta E = (S_p - 0.25S_p)nT \tag{4.4}$$

Let us assume that the capacitor dealing with this change in energy is allowed to change its voltage from $0.9V_{L-pk}$ to $1.1V_{L-pk}$, i.e.,

$$\Delta E = \frac{1}{2}C_{dc}[(1.1V_{L-pk})^2 - (0.9V_{L-pk})^2] \tag{4.5}$$

Combining (4.4) and (4.5), we get,

$$\frac{1}{2}C_{dc}[(1.1V_{L-pk})^2 - (0.9V_{L-pk})^2] = (S_p - 0.25S_p)nT$$

Assuming that the transients are handled within 1 cycle,

$$C_{dc} = \frac{2 \times (1 - 0.25) \times 15000 \times 0.02}{(1.1^2 - 0.9^2) \times (230 \times \sqrt{2})^2} = 10mF \tag{4.6}$$

Hence, the value of DC link capacitance is chosen as 10,000 μF.

4.7 Maximum Rated Filter Current, I_{f-max}

The maximum filter current is determined by the best compensation required in the worst-case situation in order to fully meet the compensation goals. The fundamental goal of creating a filter is to achieve pure harmonic cancellation as well as full reactive power compensation, which can be accomplished with the same circuit or separately [23]. Although full reactive power compensation (or any reactive power compensation) is not required for marine systems because ships have dedicated generators and good pf is not required, the system can be designed for the worst-case scenario with full reactive power compensation to identify the maximum rating requirement. The compensator can then be de-rated based on user requirement or depending on the size constraints, space availability, weight constraints or many other factors contributing to effective design of a marine platform. The design directorates might make this option throughout the ship design stage based on the needs for a given ship class.

For the present system under consideration, as a proof of concept, the filter is designed for pure harmonic cancellation and full reactive power compensation to the extant possible. As stated in Chapter 2, the filter is designed for a 1.37 kW, 230 V, 0.85 pf electric propulsion system, driven by a variable frequency drive. The rms value of per phase reactive component of current generated by the source, if the system is left

uncompensated by filter, is given by,

$$|\overline{I}_{reac}| = \frac{Q_L}{|\overline{\overline{V}^*}|} \tag{4.7}$$

For the system under consideration, Q_L is taken as 6 kVAR which includes the reactive power requirement of propulsion motor and other loads connected to the generator. Therefore, the per phase reactive current component can be calculated as,

$$|\overline{I}_{reac}| = \frac{6 \times 10^3}{3 \times 230} = 8.7A \tag{4.8}$$

Therefore, the rms value of per phase reactive current that needs to be supplied by the compensator can be approximated as, $|\overline{I}_{f-reac}|$ = 9 A.

Similarly, for pure harmonic cancellation at rated current, a certain maximum THD needs to be pre-defined. For the system under consideration, it is assumed that the compensator needs to generate harmonic currents for a maximum THD of 30% at full load current. For determining the harmonic currents, the maximum rated load current needs to be computed. The per phase rms value of load current is computed as,

$$I_L = \frac{P}{\sqrt{3} \times V_L \times pf}$$

$$I_L = \frac{1.37 \times 10^3}{3 \times 230 \times 0.85} = 2.34A \tag{4.9}$$

Assuming a certain maximum THD present in the load current, the value of harmonic current is computed as,

$$I_{har} = THD \times I_L \tag{4.10}$$

For the system under consideration, since the maximum assumed THD is 30%, the required harmonic current to be generated by the compensator is given as,

$$I_{f-har} = 0.3 \times 2.34 = 0.702A \tag{4.11}$$

Hence, the rms value of harmonic currents required to be generated by the compensator is approximated as I_{f-har} = 0.702 A.

Since the compensator is expected to generate a current for compensating both harmonics as well as reactive power, the total rms current to be generated by the filter is given as,

$$I_{f-max} = \sqrt{I_{f-reac}^2 + I_{f-har}^2} \tag{4.12}$$

i.e.,

$$I_{f-max} = \sqrt{9^2 + 0.702^2} = 9.03A \tag{4.13}$$

Hence, the total filter current to be generated for pure harmonic cancellation and full reactive compensation for the system under consideration is approximated to I_{f-max} = 10A. This is the maximum rated filter current that flows through the ac side of inverter.

4.8 Maximum Filter Power Rating, S_f

According to (4.13), the rated filter current supplied to the grid through the coupling passive filter is 10A and hence, the rating of filter is given as,

$$S_f = \sqrt{3} \times V_L \times I_{f-max} \tag{4.14}$$

i.e.,

$$S_f = \sqrt{3} \times 400 \times 10 = 7kVA \tag{4.15}$$

4.9 Selection of Hysteresis Band, h

As explained in Chapter 3, hysteresis band controller is selected as it is simple, easy to implement and has fast response, when compared to other current controllers [28]. The hysteresis band is selected based on the amount of ripple percentage allowed to be present in the actual filter current waveform so that it follows the reference current with pre-defined ripple. In general, 5-15$\%$ ripple is allowed in the current waveform for ideal compensation [22]. Additionally, it is necessary to consider the maximum switching frequency as well as the total inductance of coupling passive filter, while designing the

hysteresis band. The equation for determining the value of hysteresis band is given as,

$$2h = \%I_{ripple} \times I_{f-max} \tag{4.16}$$

where $\%I_{ripple}$ is the maximum allowable ripple percentage in current waveform. For the present study, the maximum ripple percentage is assumed to be 10%, i.e.,

$$2h = 0.1 \times 10 = 1A \tag{4.17}$$

Various active filter parameters computed in Sections 4.5 to 4.9 are as shown in the table 4.2.

Table 4.2: Active filter parameters

Parameters	**Values**
DC link voltage, V_{dc}	300
DC link capacitance, C_{dc}	10000 μ F
Rated filter current, I_{f-max}	10 A
Max current ripple	1A
Filter rating, S_f	7kVA
Hysteresis band, 2h	1A
Max switching frequency	10 kHz

4.10 Shunt Capacitor Parameters

As discussed in Chapter 3, design of shunt Capacitor C_{sh} is undertaken in such a way that the capacitor C_{sh} will not resonate with the source reactance at fundamental frequency. Here source reactance is calculated as follows,

$$X_s = 2 \times \pi \times 50 \times 31.8 \times 10^3 \tag{4.18}$$

On calculating we get X_s=10 Ω. Therefore, the capacitance for resonating at fundamental frequency, i.e., C_{sho} can be calculated using (3.49) as,

$$C_{sho} = \frac{1}{(2 \times \pi \times 50)^2 \times 31.8 \times 10^{-3}} \tag{4.19}$$

Thus we get C_{sho} as 318μF. Here as defined in Chapter 3, the values of C_{sh} is taken very lesser than C_{sho}. Calculating in this way we choose C_{sh} as 50μF.

4.11 Coupling Passive Filter Parameters

The design of passive filter is explained in detail in Chapter 3 Section 3.7. Initially, the series inductance L_f is designed using (4.20) as,

$$L_f = \frac{1.6 \times 230 \times \sqrt{2}}{4 \times 10000 \times 0.5} \tag{4.20}$$

here, V_m is taken as 230$\sqrt{2}$,f$_{swmax}$ is taken as 10000 and h is taken as 0.5. Thus we get the value of L_f as 26 mH.

Once the series inductance is designed, the series capacitor C_f is designed based on the requirement of reactive power injection into the grid. The shunt filter current must supply the requisite load reactive current in order to attain unity power factor, i.e., the imaginary part of the filter current must match the imaginary portion of the load current. Based on this condition (3.54) is derived in Chapter 3. For solving the above equation the lowest load impedance is taken as impedance in phase *a*, i.e., R_l+jX_l = 34+j47.5 Ω. Further the value of V_{inv1} is computed based on (3.55) as

$$V_{inv1} = \frac{0.612 \times 300}{\sqrt{3}} = 106V \tag{4.21}$$

Accordingly, on substituting values in (3.54) we get,

$$\frac{230 \times 47.5}{34^2 + 47.5^2} = \frac{106 - 230}{(2 \times \pi \times 50 \times 26 \times 10^{-3}) - X_{cf}} \tag{4.22}$$

On solving the above equation we get, X_{cf} = 46.9 Ω. From this value of X_{Cf}, C_f can be calculated as follows:-

$$C_f = \frac{1}{2 \times \pi \times 50 \times 46.9} \tag{4.23}$$

Thus, we get the value of C_f as 67.8 μF. This can be approximated as 65 μF.

Various coupling passive filter and shunt capacitor parameters are as shown in the table 4.3

Table 4.3: Coupling filter and shunt capacitor parameters

Parameters	**Values**
Series inductance, L_f	26 mH
Series capacitance, C_f	65 μ F
Shunt capacitance, C_{sh}	50 μ F

4.12 Selection of PI Controller Constants, $k_p^{'}$, $k_i^{'}$

The design of PI controller for maintaining a constant DC link voltage is explained in detail in Chapter 3 Section 3.4. The value of proportional gain can be determined by substituting the value of C_{dc} and f_r in (3.43). Assuming that the ripple frequency is four times that of the supply frequency, the proportional gain can be determined as,

$$k_p^{'} = \frac{200 \times 10000 \times 10^{-6}}{2} = 1 \tag{4.24}$$

Once the $k_p^{'}$ value is determined, the $k_i^{'}$ value can be computed by substituting the value of $k_p^{'}$ in (3.44) as,

$$k_i^{'} = \frac{1}{2} = 0.5 \tag{4.25}$$

Even though the $k_p^{'}$, $k_i^{'}$ values determined as per (4.24) and (4.25) are good enough for ideal compensation, the values can be further increased to improve the transient response, with the overshoot values restricted to acceptable limits. However, for the same performance, the conventional PI controller has higher gain values when compared to a fast acting controller being used in the present study.

4.13 Summary

In this chapter, the values of source and load characteristics relevant to a maritime platform were used to calculate various system parameters. The characteristics of the inverter and passive filter were chosen based on the design considerations outlined in Chapter 3 expanded for a marine platform. The simulation results and observations are reported in the following chapter, together with the system parameter values derived in this chapter.

CHAPTER 5

RESULTS AND OBSERVATIONS

5.1 Introduction

The proposed hybrid filter for an IFEP propulsion system as shown in Fig. 3.6 (repeated below as Fig. 5.1) is considered for simulation studies done in MATLAB SIMULINK. The detailed parameters of the source and propulsion system as shown in Table 4.1 in Chapter 4 is repeated below in Table 5.1 for ready reference. The system parameters are chosen based on the design calculations performed in different sections of Chapter 4. A propulsion system with a 1.37 kW, 0.85 pf induction motor fed through a rectifier-inverter assembly, as well as unbalanced loads across three phases, make up the load.

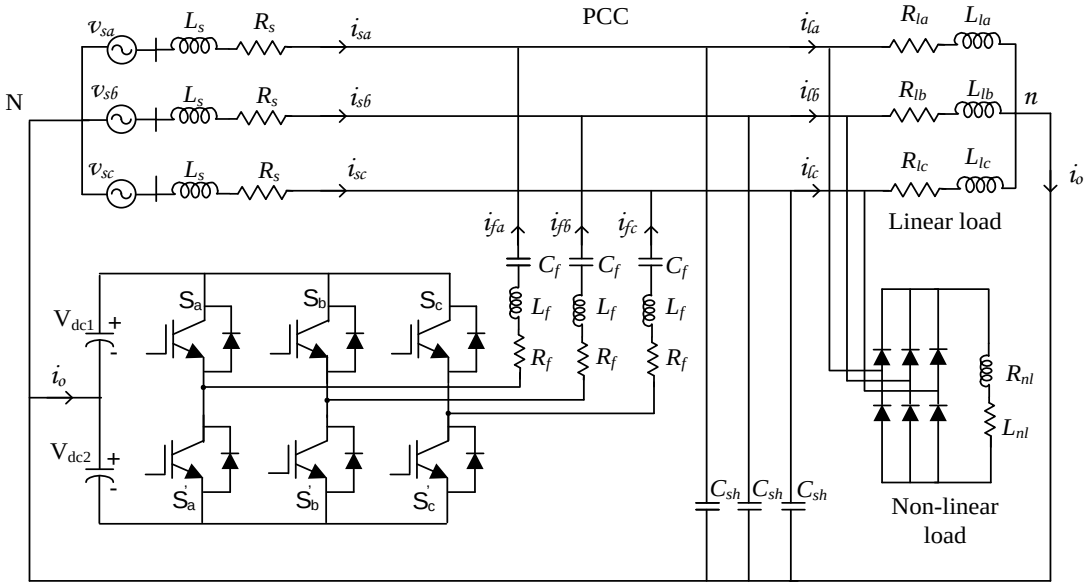

Fig. 5.1: DSTATCOM with interfacing passive filter

Table 5.1: Source and load parameters

Parameters	**Values**
Source voltage (Phase to neutral)	230 V
SC level	15 kVA
Source reactance	10 Ω
Source resistance	1 Ω
Source inductance	31.8 mH
Load Active Power	1.37 kW
Load power factor	0.85
Load Reactive Power	0.86 kVAr
Phase *a* other load	34+j47.5 Ω
Phase *b* other load	81+j39.6 Ω
Phase*cc* other load	31.5+j70.9 Ω

5.2 Results

The source line voltage, when load is directly connected to the source without the employment of a compensator, is as shown in Fig. 5.2.

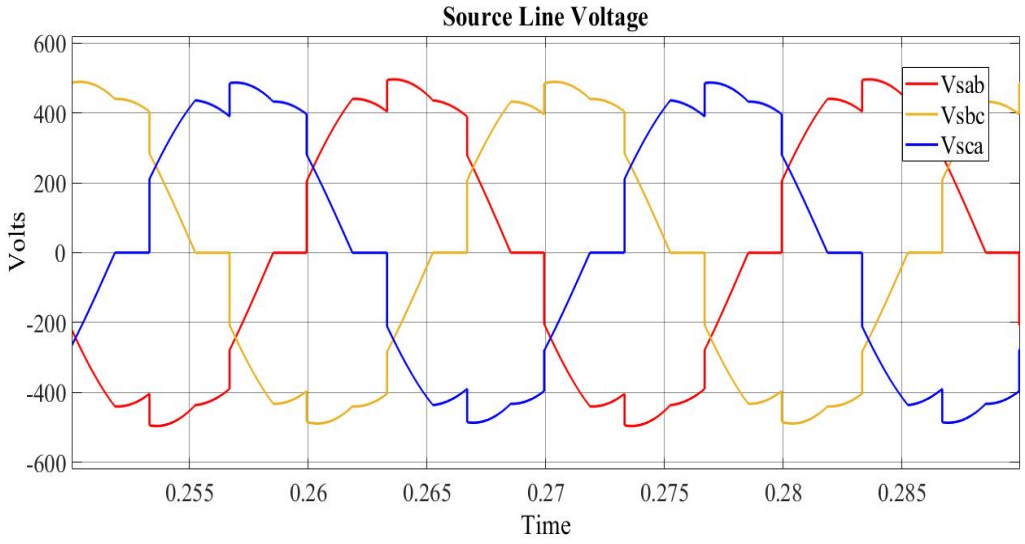

Fig. 5.2: Source voltage without filter

Similarly, the source line current waveforms, when load is directly connected to the source without the employment of a compensator, is also shown in Fig. 5.3. It is quite evident from the waveforms in Figs. 5.2 and 5.3 that the source voltages and currents

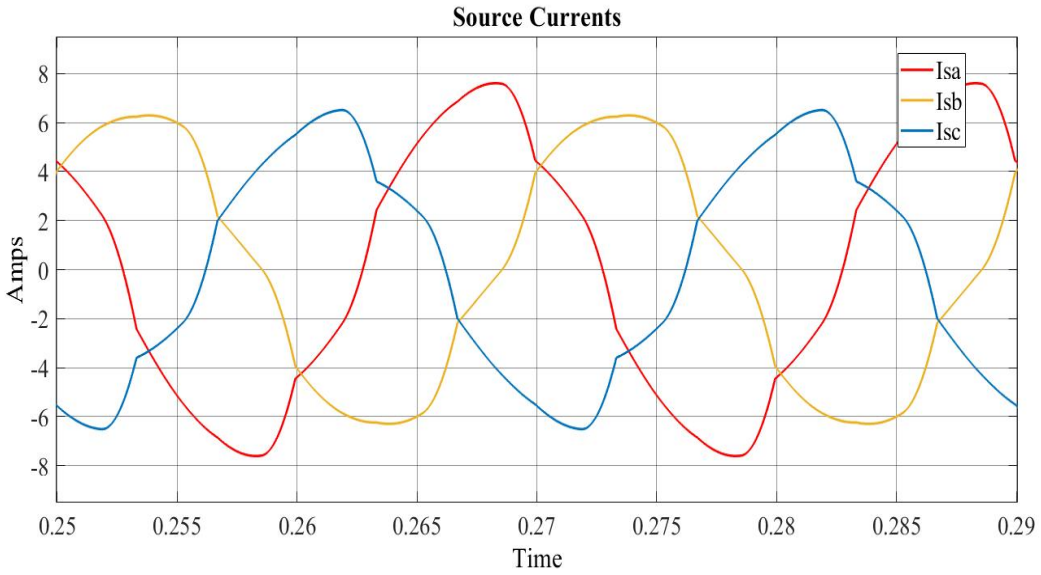

Fig. 5.3: Source current without filter

are quite distorted due to the use of non-linear components in the load. Further the source current is unbalanced due to the unbalance in loads. The harmonic spectrum for source voltage and current in R phase, depicting the fundamental and the THD value, is shown in Figs. 5.4a and 5.4b respectively. The THD values of source voltage and current are 12.52% and 7.95% respectively. Since the THD values are outside the limits specified in IEEE 519-2014, it is essential to employ compensation techniques to improve the power quality. Hence, a hybrid filter was chosen for the propulsion system under consideration.

For analysis purpose and for better understanding of the benefits of a hybrid filter, a simulation was undertaken with a passive filter alone as specified in Chapter 4 . The results of the same are shown in Fig. 5.5. The source current waveforms have been improved. However, the unbalance in the waveforms still persists. The THD values of the source voltage and source currents are shown in Figs. 5.6a and 5.6b. It is seen that the source voltage and current THD values have improved from 12.52% and 7.95% to 5.47% and 4.73% respectively. Though the current THD values are within the limits specified in IEEE 519-2014, the voltage THD values can still be improved. Further the unbalance in current waveform also can be improved. Hence, we go for a hybrid filter.

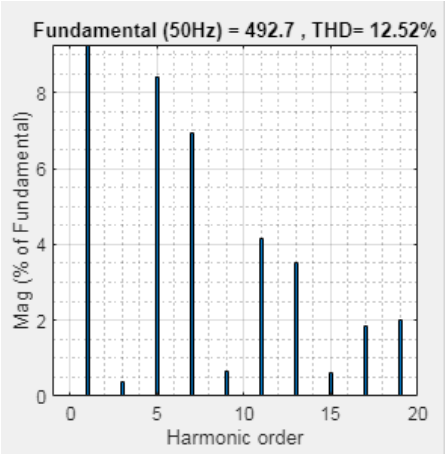

(a) Source line voltage (R-Phase)

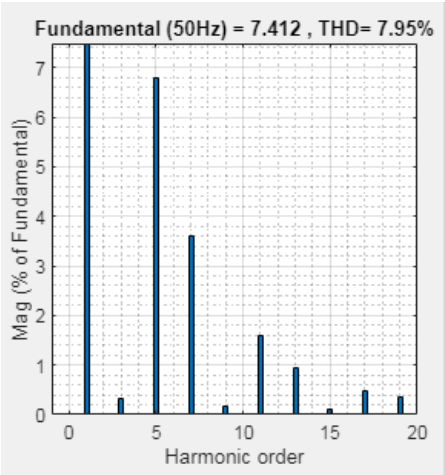

(b) Source line current (R-Phase)

Fig. 5.4: Harmonic spectrum w/o filter

Post implementation of an active filter with a coupling passive filter to form a hybrid filter and with a shunt capacitor with parameter design as specified in various sections in Chapter 4, the source line voltage and current waveforms have improved with better THD values, as shown in Fig. 5.7. The source voltage and current THD values have improved from 12.52% and 7.95% to 2.59% and 3.02% respectively.

The harmonic spectrum of source line voltage and current, depicting the peak magnitude of fundamental voltage and current along with their respective THD values are shown in Figs. 5.8a and 5.8b. It is evident that the current and voltage harmonics have significantly reduced across the frequency spectrum with values much within limits specified by IEEE standards.

Here, instantaneous symmetrical component theory is used for reference filter current generation, which is explained in detail in Chapter 3. In order to ensure ideal compensation, it is essential that the actual filter currents generated by the compensator follows the reference filter currents generated analytically from the source line voltages and the average load power and power losses in the compensator.

Because the source voltage contains harmonics, it is critical to extract the fundamental components of source line voltages for analytical calculations. If the computations are done with a source voltage waveform that contains harmonics, the compensation will be insufficient, and the compensator will be unsuitable for harmonic cancellation.

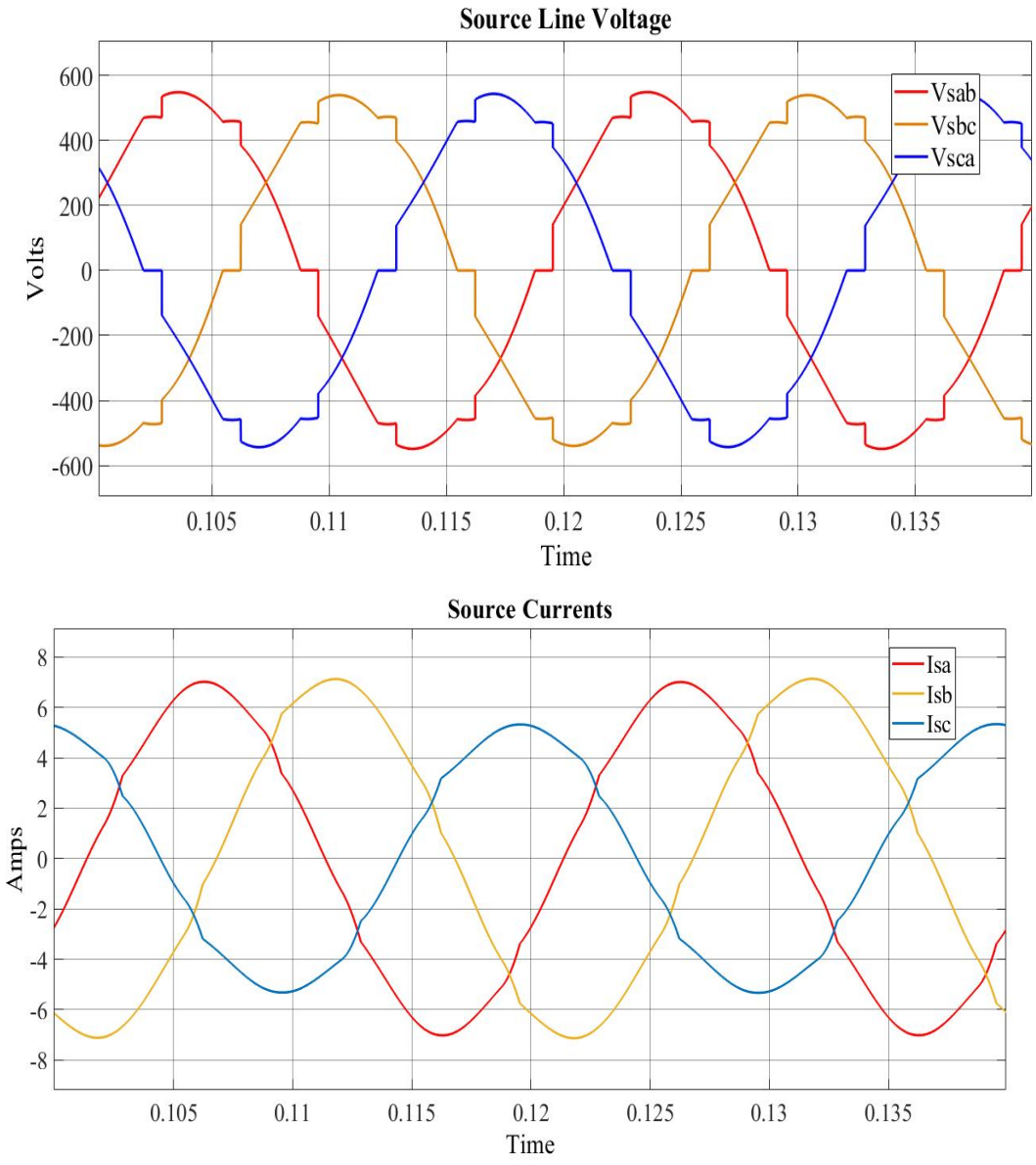

Fig. 5.5: Source line voltage and current waveforms with passive filter alone

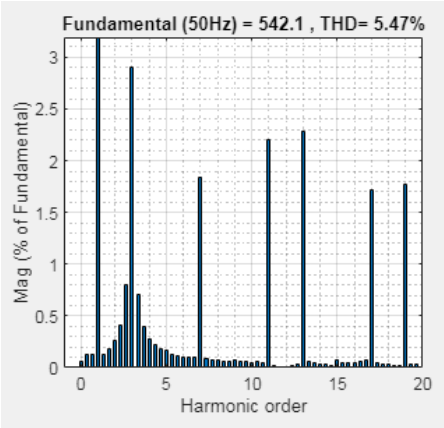

(a) Source line voltage (R-Phase)

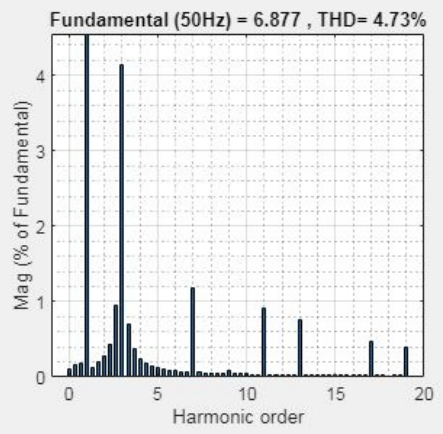

(b) Source line current (R-Phase)

Fig. 5.6: Harmonic spectrum with passive filter alone

For average load power calculations, the fundamental positive sequence components of load voltages and currents are also necessary. Even though the calculation of fundamental components takes a few cycles, it is necessary for error-free calculation of reference filter currents. When simulations were conducted directly with source line voltages, harmonics were detected in the output waveform that were not present in the original uncompensated waveform. This indicates that the compensator is pumping harmonics into the grid as a result of incorrect reference filter current calculations.

A hysteresis band current controller, which is perfectly designed to suit the THD needs of the input and the reactive power requirements of the load, is used to ensure that the real filter current follows the reference filter current. The reference filter currents and the actual filter currents are as shown in Fig. 5.9.

It is evident from Fig 5.9 that the actual current is following the reference filter current and hence, can state that the current controller is working satisfactorily with the set value of hysteresis band designed in Chapter 4 Section 4.9. Further decrease in the value of hysteresis band does not improve the performance of the controller considerably, but requires higher switching frequency, resulting in higher switching losses. Hence, the analytical value of hysteresis band, computed in Chapter 4 Section 4.9, is practically verified to be an ideal value using simulation studies.

The excellent filter current following with reduced current ripples is additionally attributed to the effective design of passive filter and shunt capacitor parameters, un-

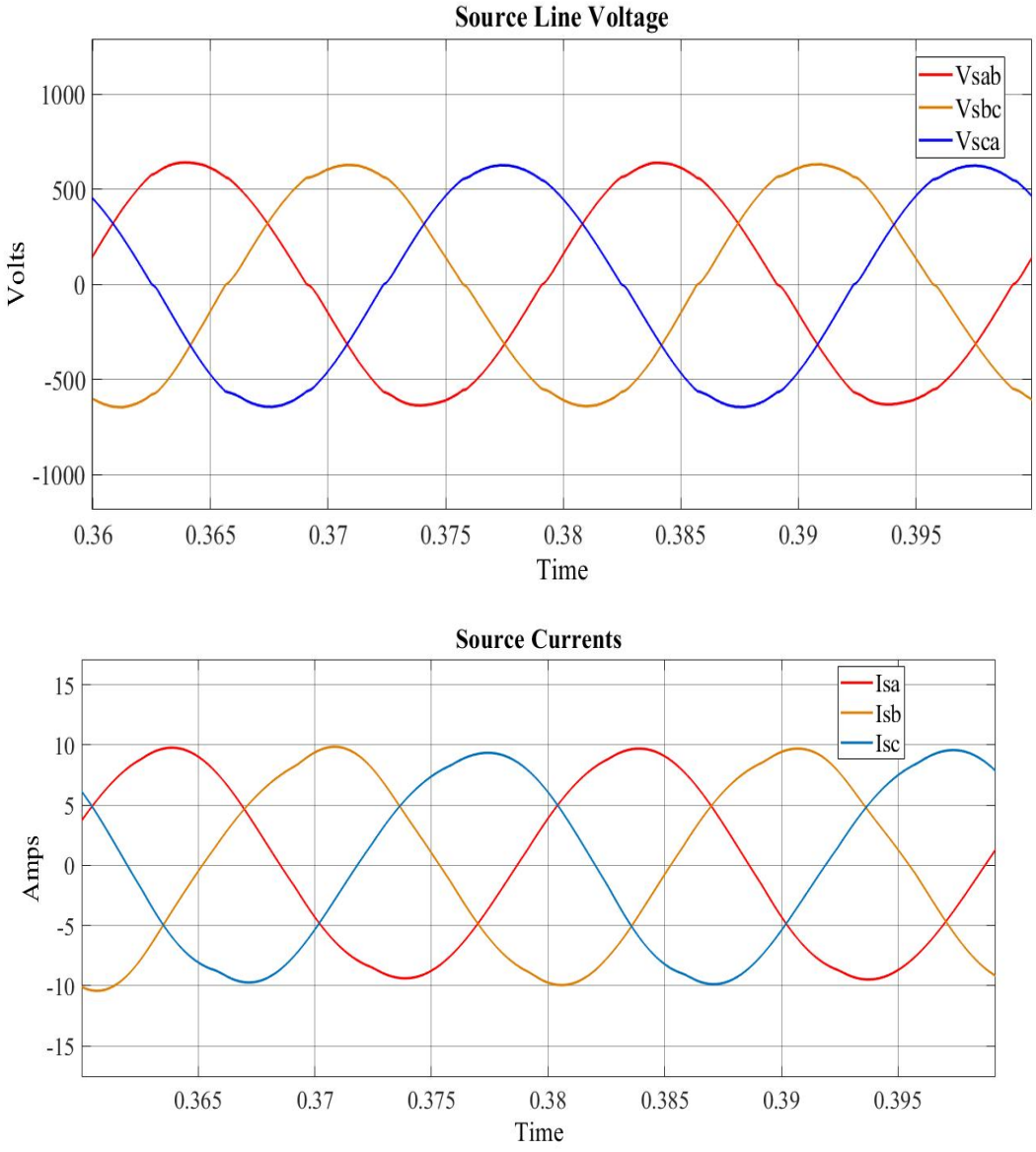

Fig. 5.7: Source line voltage and current waveforms with hybrid filter

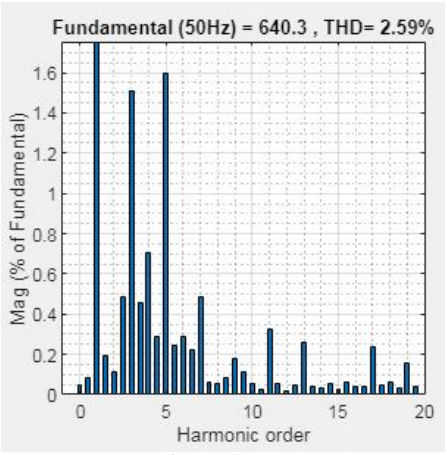

(a) Source line voltage (R-Phase)

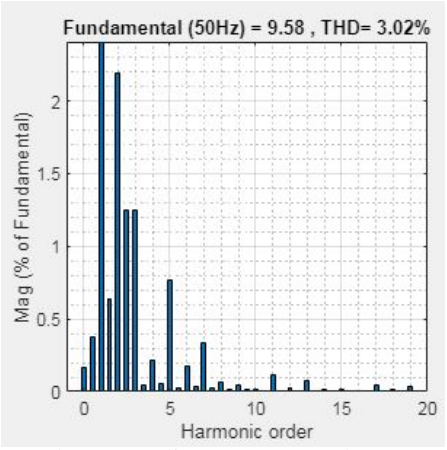

(b) Source line current (R-Phase)

Fig. 5.8: Harmonic spectrum with hybrid filter

dertaken in Chapter 4. Even though the current ripples can be reduced with a single coupling inductor, the inductance value required will be high, which in turn increases the voltage drop across the inductor. Further, with the use of hybrid filter it is noticed that the DC link voltage has been reduced.

The active filter voltage and the source capacitance values were determined in Chapter 4 Sections 4.5 and 4.6 respectively. The filter voltage is maintained at constant value by using a PI controller, the design of which is specified in Chapter 4 Section 4.12. The controller performance can be analysed by checking the filter source voltage waveform, which is shown in Fig. 5.10.

It is evident from Fig. 5.10 that, with the pre-defined value of $k_p^{'}$ and $k_i^{'}$ as computed in Chapter 4 Section 4.12, the response is slow. However, the slow response is mainly attributable to the slow computation of average load power and reference filter current, as it requires evaluation of fundamental positive sequence components of voltage and current waveform. Even though the computation of fundamental positive sequence of voltage and current takes time, it is essential to use these quantities for error-free evaluation of filter reference currents and average load waveforms.

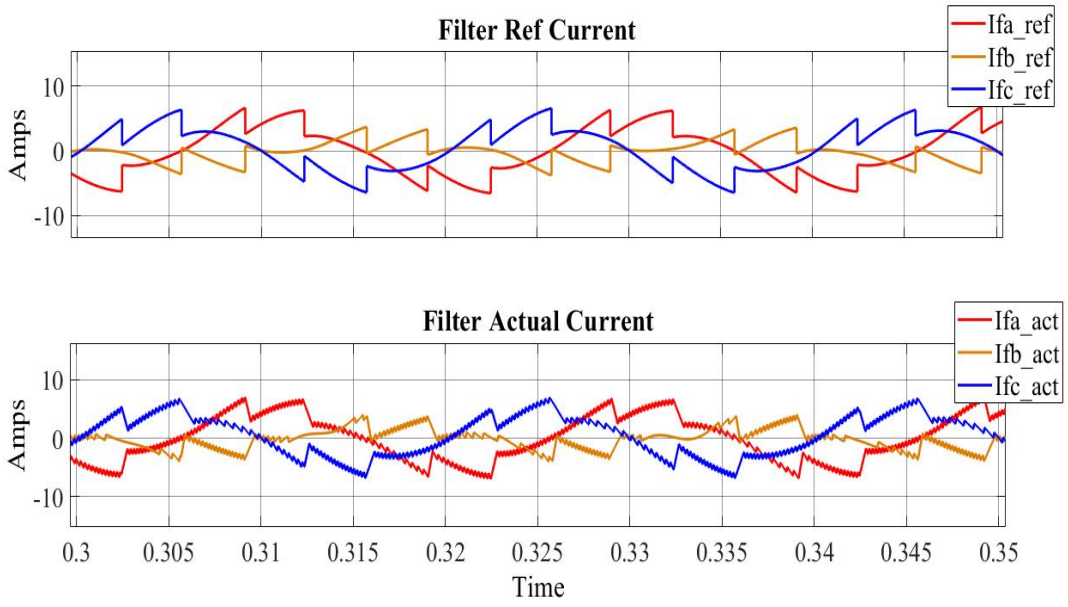

Fig. 5.9: Reference and actual filter currents

5.3 Summary

The results obtained from the simulation of shunt active power filter for harmonic cancellation and reactive power compensation for a non-linear propulsion motor load was presented in this chapter. It is observed that there is considerable improvement in voltage and current THDs after implementation of active filter and the values are well within the limits specified in IEEE std. 519-2014 [9]. The results are satisfactory even at lower values of V_{dc}.

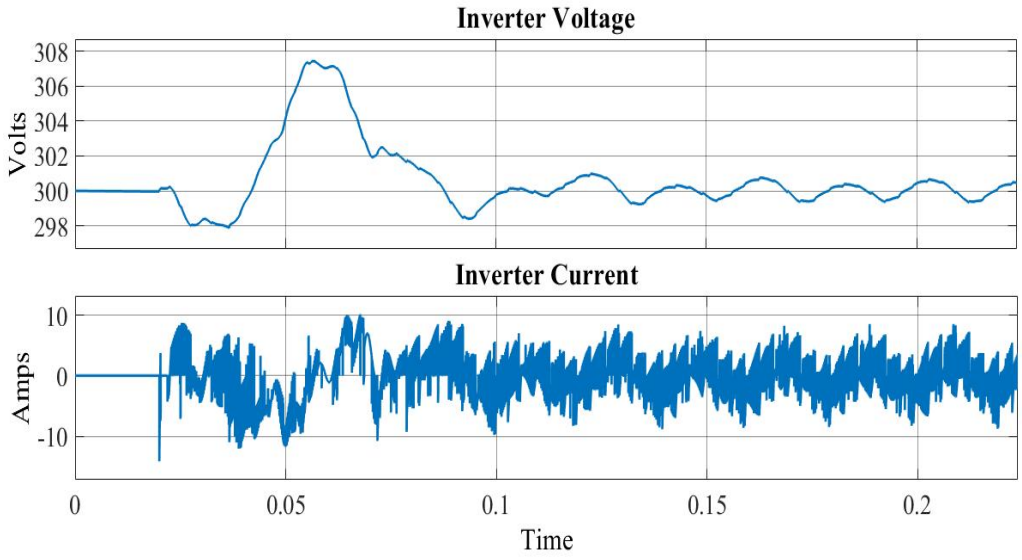

Fig. 5.10: Active filter DC link voltage and current

CHAPTER 6

CONCLUSION

6.1 Project Summary

Simulation experiments have successfully proven the implementation of a hybrid active power filter for a non-linear VFD powered propulsion motor load used onboard an integrated complete electric propulsion ship for harmonic cancellation and reactive power correction. The use of a passive LC filter in series with an active filter to form a hybrid filter, as well as a shunt capacitance for filtering switching harmonics, has been found to offer superior filter output at lower DC link voltages. The THDs of the source voltage/current have improved due to the usage of filter. Various parameter designs for effective compensation have been shown to be perfect, and simulation results have proven promising. Because the creation of reference source currents necessitates a harmonic-free source voltage waveform, calculations using fundamental positive sequence voltage values are required for error-free reference current computation. Even though the compensator takes a few cycles to enable the source to create sinusoidal source current, this is acceptable for a maritime platform because electric propulsion is typically utilised for routine voyages that do not necessitate a faster response. Other loads linked to the PCC may perform worse during the settling time, but this can be overlooked because the settling period is short. Furthermore, the loads connected during routine voyages are of low criticality, with the exception of a few crucial loads such as steering gear, navigation radars, and communication equipment, which can function satisfactorily even with low-quality source voltages for a few cycles.

With improved voltage THD, the system integrator's job becomes easier with other loads that require fewer complicated filters at their input, resulting in higher power quality for these loads at lower individual system costs. Individual systems can also be smaller, freeing up space for additional shipboard equipment, living area, and leisure

facilities. Furthermore, the system is not susceptible to the spread of passive filter drawbacks. With this topology, several of the shortcomings of an active filter, such as significant switching losses and conduction losses, have been mitigated. Future research and development in the field of power electronics, on the other hand, may be able to reduce it even more. Hence, the major conclusions from the project can be listed as follows.

- With appropriately designed harmonic compensation system for power quality improvement, an IFEP ship can prove to be one of the best replacement for traditional propulsion ships.
- An active power filter can be seen as the finest solution for an IFEP based marine power system because of its improved characteristics and superior performance over a large load range.
- Performance of hybrid filter with shunt capacitance topology at reduced DC link voltage is found to be superior when compared with a simple active filter topology.
- Future researches and developments in the field of power electronics can ensure realisation of more compact, robust and cost effective topologies for IFEP based marine power systems.

6.2 Future Scope

The project has a lot of room for growth, especially in terms of developing the hardware setup for the established simulation approach. Only a prototype model has been created thus far to demonstrate the concept. However, as a next step towards complete project realisation, the creation of a realistic model as well as hardware is required. Onboard a ship, space is limited, hence the size of the system should be limited by the amount of space available for setting up the compensator. To assess an active filter's efficiency aboard, the benefits must be weighed against the size and cost considerations. Also, because a ship is prone to extreme roll and pitch in bad weather, shock and vibration must be taken into account while building a functional onboard system. Furthermore, a practical configuration may necessitate further tuning of the design for optimal installation onboard, which must be examined before the model is developed. Furthermore, literature suggests that using a hybrid active power filter in parallel with a static VAR

compensator can improve harmonic cancellation and reactive power compensation performance. Such a filter can dynamically adjust reactive power and ensure that the VSI rating is reduced in terms of voltage and current. This can help save money on the complete filter setup. As a result, if a hybrid active power filter in parallel with a Static VAR compensator can deliver greater output at a reduced size/cost, it may be considered for use onboard an electric propulsion ship.

REFERENCES

[1] K. Chetan, H. Goel, O. Sharma, and R. Vishwakarma, "Electric Propulsion - Implementation and Way Ahead," Tech. Rep. file/2127, IN, IHQ MoD(N), New Delhi, 2019.

[2] D. Kumar and F. Zare, "A comprehensive review of maritime microgrids: System architectures, energy efficiency, power quality, and regulations," *IEEE Access*, vol. 7, pp. 67249–67277, 2019.

[3] C. Hodge, "Modern applications of power electronics to marine propulsion systems," in *Proceedings of the 14th International Symposium on Power Semiconductor Devices and Ics*, pp. 9–16, 2002.

[4] Y. Terriche, M. U. Mutarraf, M. Mehrzadi, C. L. Su, J. M. Guerrero, J. C. Vasquez, D. Kerdoun, and A. Alonso, "Power quality and voltage stability improvement of shipboard power systems with non-linear loads," in *2019 IEEE International Conference on Environment and Electrical Engineering and 2019 IEEE Industrial and Commercial Power Systems Europe (EEEIC / I CPS Europe)*, pp. 1–6, 2019.

[5] B. D. Reddy, S. Lingeshwaren, M. Chai, Y. D. Babu, P. Chuhan, S. R. Kamala, S. Panda, D. Wu, and X. Q. Chen, "Investigations on lvac architectures of diesel electric propulsion based marine vessels for improved power quality and reliability," in *2016 IEEE 8th International Power Electronics and Motion Control Conference (IPEMC-ECCE Asia)*, pp. 2854–2858, 2016.

[6] J. Mindykowski, "Power quality on ships: Today and tomorrow's challenges," in *2014 International Conference and Exposition on Electrical and Power Engineering (EPE)*, pp. 001–018, 2014.

[7] V. Arcidiacono, S. Castellan, R. Menis, and G. Sulligoi, "Integrated voltage and reactive power control for all electric ship power systems," in *International Symposium on Power Electronics, Electrical Drives, Automation and Motion, 2006. SPEEDAM 2006.*, pp. 878–882, 2006.

[8] "IEEE recommended practice for electric installations on shipboard," *IEEE Std 45-2002 (Revision of IEEE Std 45-1998)*, pp. 1–272, 2002.

[9] "IEEE recommended practice and requirements for harmonic control in electric power systems," *IEEE Std 519-2014 (Revision of IEEE Std 519-1992)*, pp. 1–29, 2014.

[10] S. V. Giannoutsos and S. N. Manias, "A systematic power-quality assessment and harmonic filter design methodology for variable-frequency drive application in marine vessels," *IEEE Transactions on Industry Applications*, vol. 51, no. 2, pp. 1909–1919, 2015.

[11] S. Puthalath and G. Bhuvaneswari, "Power quality enhancement and renewable energy integration in ship's distribution grid," in *2018 IEEMA Engineer Infinite Conference (eTechNxT)*, pp. 1–6, 2018.

[12] N. K. Bett, C. C. Maina, and P. K. Hinga, "New approach for design of shunt active power filter for power quality improvement in a three phase three wire system," in *2020 IEEE PES/IAS PowerAfrica*, pp. 1–4, 2020.

[13] V. F. Corasaniti, M. B. Barbieri, P. L. Arnera, and M. I. Valla, "Hybrid power filter to enhance power quality in a medium-voltage distribution network," *IEEE Transactions on Industrial Electronics*, vol. 56, no. 8, pp. 2885–2893, 2009.

[14] H. Akagi, "New trends in active filters for power conditioning," *IEEE transactions on industry applications*, vol. 32, no. 6, pp. 1312–1322, 1996.

[15] H. Akagi, "Active harmonic filters," *Proceedings of the IEEE*, vol. 93, no. 12, pp. 2128–2141, 2005.

[16] H. Akagi, S. Srianthumrong, and Y. Tamai, "Comparisons in circuit configuration and filtering performance between hybrid and pure shunt active filters," in *38th IAS Annual Meeting on Conference Record of the Industry Applications Conference, 2003.*, vol. 2, pp. 1195–1202 vol.2, 2003.

[17] R. Inzunza and H. Akagi, "A 6.6-kv transformerless shunt hybrid active filter for installation on a power distribution system," *IEEE Transactions on Power Electronics*, vol. 20, no. 4, pp. 893–900, 2005.

[18] J. L. Afonso, M. S. Freitas, and J. S. Martins, "pq theory power components calculations," in *2003 IEEE International Symposium on Industrial Electronics (Cat. No. 03TH8692)*, vol. 1, pp. 385–390, IEEE, 2003.

[19] E. H. Watanabe, M. Aredes, and H. Akagi, "The pq theory for active filter control: some problems and solutions," *Sba: Controle & Automação Sociedade Brasileira de Automatica*, vol. 15, no. 1, pp. 78–84, 2004.

[20] M. Kumar, "NPTEL course on power quality in power distribution systems," 2012.

[21] M. K. Mishra and K. Karthikeyan, "Design and analysis of voltage source inverter for active compensators to compensate unbalanced and non-linear loads," in *2007 International Power Engineering Conference (IPEC 2007)*, pp. 649–654, 2007.

[22] M. K. Mishra and K. Karthikeyan, "An investigation on design and switching dynamics of a voltage source inverter to compensate unbalanced and nonlinear loads," *IEEE Transactions on Industrial Electronics*, vol. 56, no. 8, pp. 2802–2810, 2008.

[23] U. K. Rao and M. K. Mishra, "Control strategies for load compensation using instantaneous symmetrical component theory under different supply voltages," in *2007 International Power Engineering Conference (IPEC 2007)*, pp. 596–601, IEEE, 2007.

[24] N. M. Ismail and M. K. Mishra, "Study on the design and switching dynamics of hysteresis current controlled four-leg voltage source inverter for load compensation," *IET power electronics*, vol. 11, no. 2, pp. 310–319, 2018.

[25] J. Suma and M. K. Mishra, "Instantaneous symmetrical component theory based algorithm for characterization of three phase distorted and unbalanced voltage sags," in *2013 IEEE International Conference on Industrial Technology (ICIT)*, pp. 845–850, IEEE, 2013.

[26] C. Kumar and M. K. Mishra, "Energy conservation and power quality improvement with voltage controlled dstatcom," in *2013 Annual IEEE India Conference (INDICON)*, pp. 1–6, IEEE, 2013.

[27] C. Kumar, M. K. Mishra, and M. Liserre, "Design of external inductor for improving performance of voltage-controlled dstatcom," *IEEE transactions on Industrial Electronics*, vol. 63, no. 8, pp. 4674–4682, 2016.

[28] M. K. Mishra and K. Karthikeyan, "A fast-acting dc-link voltage controller for three-phase dstatcom to compensate ac and dc loads," *IEEE transactions on power delivery*, vol. 24, no. 4, pp. 2291–2299, 2009.

[29] D. M. Ingram and S. D. Round, "A novel digital hysteresis current controller for an active power filter," in *Proceedings of Second International Conference on Power Electronics and Drive Systems*, vol. 2, pp. 744–749, IEEE, 1997.

[30] C.-T. Pan and T.-Y. Chang, "An improved hysteresis current controller for reducing switching frequency," *IEEE Transactions on Power Electronics*, vol. 9, no. 1, pp. 97–104, 1994.

[31] M. Kale and E. Ozdemir, "A novel adaptive hysteresis band current controller for shunt active power filter," in *Proceedings of 2003 IEEE Conference on Control Applications, 2003. CCA 2003.*, vol. 2, pp. 1118–1123, IEEE, 2003.

[32] S. Jayalath and M. Hanif, "Generalized lcl-filter design algorithm for grid-connected voltage-source inverter," *IEEE Transactions on Industrial Electronics*, vol. 64, no. 3, pp. 1905–1915, 2016.

[33] M. Liserre, F. Blaabjerg, and S. Hansen, "Design and control of an lcl-filter-based three-phase active rectifier," *IEEE Transactions on industry applications*, vol. 41, no. 5, pp. 1281–1291, 2005.

[34] C. Kumar, M. K. Mishra, and M. Liserre, "Lcl filter based upqc configuration for power quality improvement," in *2016 IEEE Power and Energy Society General Meeting (PESGM)*, pp. 1–5, IEEE, 2016.

[35] R. Pena-Alzola, M. Liserre, F. Blaabjerg, M. Ordonez, and Y. Yang, "Lcl-filter design for robust active damping in grid-connected converters," *IEEE Transactions on Industrial Informatics*, vol. 10, no. 4, pp. 2192–2203, 2014.

[36] A. Reznik, M. G. Simões, A. Al-Durra, and S. Muyeen, "lcl filter design and performance analysis for grid-interconnected systems," *IEEE transactions on industry applications*, vol. 50, no. 2, pp. 1225–1232, 2013.

[37] S. B. Karanki, N. Geddada, M. K. Mishra, and B. K. Kumar, "A dstatcom topology with reduced dc-link voltage rating for load compensation with nonstiff source," *IEEE Transactions on Power Electronics*, vol. 27, no. 3, pp. 1201–1211, 2012.

[38] L. Wang, C.-S. Lam, and M.-C. Wong, "Hybrid structure of static var compensator and hybrid active power filter (svc//hapf) for medium-voltage heavy loads compensation," *IEEE Transactions on Industrial Electronics*, vol. 65, no. 6, pp. 4432–4442, 2018.

[39] G. Feix, S. Dieckerhoff, J. Allmeling, and J. Schonberger, "Simple methods to calculate igbt and diode conduction and switching losses," in *2009 13th European Conference on Power Electronics and Applications*, pp. 1–8, IEEE, 2009.